A STUDY INTO THE MECHANISM(S) FOR THE ELECTROPLASTIC EFFECT IN METALS AND ITS APPLICATION TO METALWORKING, PROCESSING AND FATIGUE

Final Report

Hans Conrad

March 10, 1989

U. S. Army Research Office

ARO Proposal Number 23090–MS

ARO Funding Document DAAL03–86–K–0015

North Carolina State University
Raleigh, NC 27695

Approved for Public Release
Distribution Unlimited

UNCLASSIFIED
SECURITY CLASSIFICATION OF THIS PAGE

MASTER COPY - FOR REPRODUCTION PURPOSES

REPORT DOCUMENTATION PAGE

1a. REPORT SECURITY CLASSIFICATION: Unclassified	1b. RESTRICTIVE MARKINGS
2a. SECURITY CLASSIFICATION AUTHORITY	3. DISTRIBUTION/AVAILABILITY OF REPORT: Approved for public release; distribution unlimited.
2b. DECLASSIFICATION/DOWNGRADING SCHEDULE	
4. PERFORMING ORGANIZATION REPORT NUMBER(S)	5. MONITORING ORGANIZATION REPORT NUMBER(S): ARO 23090.17-MS
6a. NAME OF PERFORMING ORGANIZATION: N. C. State University; 6b. OFFICE SYMBOL (If applicable)	7a. NAME OF MONITORING ORGANIZATION: U. S. Army Research Office
6c. ADDRESS (City, State, and ZIP Code): Raleigh, NC 27695	7b. ADDRESS (City, State, and ZIP Code): P. O. Box 12211, Research Triangle Park, NC 27709-2211
8a. NAME OF FUNDING/SPONSORING ORGANIZATION: U. S. Army Research Office; 8b. OFFICE SYMBOL (If applicable)	9. PROCUREMENT INSTRUMENT IDENTIFICATION NUMBER: DAAL03-86-K-0015
8c. ADDRESS (City, State, and ZIP Code): P. O. Box 12211, Research Triangle Park, NC 27709-2211	10. SOURCE OF FUNDING NUMBERS: PROGRAM ELEMENT NO. / PROJECT NO. / TASK NO. / WORK UNIT ACCESSION NO.

11. TITLE (Include Security Classification)
A Study into the Mechanism(s) for the Electroplastic Effect in Metals and Its Application to Metalworking, Processing and Fatigue

12. PERSONAL AUTHOR(S)
Hans Conrad

13a. TYPE OF REPORT	13b. TIME COVERED	14. DATE OF REPORT (Year, Month, Day)	15. PAGE COUNT
Final	FROM 11/20/85 TO 11/19/88	March 10, 1989	48

16. SUPPLEMENTARY NOTATION
The view, opinions and/or findings contained in this report are those of the author(s) and should not be construed as an official Department of the Army position, policy, or decision, unless so designated by other documentation.

17. COSATI CODES		
FIELD	GROUP	SUB-GROUP

18. SUBJECT TERMS (Continue on reverse if necessary and identify by block number)
Electroplastic, electropulsing, electric field, electric current, electron wind, dislocations, plastic strain rate, recovery, recrystallization, grain growth, fatigue,(Continued)

19. ABSTRACT (Continue on reverse if necessary and identify by block number)

The effects of high-density electric current pulses and a continuous external d.c. electric field on the behavior of metals and alloys was investigated. The theoretical basis for the effects of the current pulses was considered, giving special attention to an electron wind-assisted dislocation motion. It was determined that high-density electric current pulses (10^3-10^6 A/cm^2 and ~100 μs duration) significantly increased: (a) the plastic strain rate in unidirectional straining at low homologous temperatures, (b) the fatigue life, (c) the rates of recovery and recrystallization and (d) the transformation of amorphous alloys. The increases occurred even though the current was "on" only 10^{-4} fraction of the test time. Along with the increase in rate, there generally also occurred some change in slip band structure or microstructure. It is proposed that an important factor in the effects produced by the current pulses is the influence of an electron wind on the motion of the atoms and dislocations involved.

CONTINUED ON BACK

20. DISTRIBUTION/AVAILABILITY OF ABSTRACT	21. ABSTRACT SECURITY CLASSIFICATION
☐ UNCLASSIFIED/UNLIMITED ☐ SAME AS RPT. ☐ DTIC USERS	Unclassified
22a. NAME OF RESPONSIBLE INDIVIDUAL	22b. TELEPHONE (Include Area Code) / 22c. OFFICE SYMBOL

18. superplasticity, phase transformations, amorphous alloys, quench aging, hardening, tempering.

19. → The application of a continuous external d.c. electric field of ~ 1 kV/cm retarded the following phenomena: (a) recovery and recrystallization of cold worked Al and Cu, (b) grain growth and the formation of cavities during superplastic deformation of the 7475 Al alloy, and (c) quench aging, bainite formation and tempering of steels. The electric field however increased the rates of recovery and recrystallization of the superalloy Ni_3Al and the rate of austenization of a tool steel. The effects of the field occurred throughout the bulk of the 1-3 mm thick specimens and not just at the surface, and appear to be associated with the directed atomic mobility produced by a field. Keywords: nickel; aluminum; copper; alloys; metallurgy; (RT) ←

Cont'd

Final Report
ARO Proposal Number 23090–MS
ARO Funding Document DAAL03–86–K–0015

A STUDY INTO THE MECHANISM(S) FOR THE ELECTROPLASTIC EFFECT IN METALS AND ITS APPLICATION TO METALWORKING, PROCESSING AND FATIGUE

Hans Conrad
Materials Science and Engineering Department
North Carolina State University
Raleigh, NC 27695–7907

CONTENTS

A STUDY INTO THE MECHANISM(S) FOR THE ELECTROPLASTIC EFFECT IN METALS AND ITS APPLICATION TO METALWORKING, PROCESSING AND FATIGUE

ABSTRACT

The effects of high-density electric current pulses and a continuous external d.c. electric field on the behavior of metals and alloys was investigated. The theoretical basis for the effects of the current pulses was considered, giving special attention to an electron wind-assisted dislocation motion. It was determined that high-density electric current pulses ($10^3 - 10^6$ A/cm^2 and ~ 100 μs duration) significantly **increased**: (a) the plastic strain rate in unidirectional straining at low homologous temperatures, (b) the fatigue life, (c) the rates of recovery and recrystallization and (d) the transformation of amorphous alloys. The increases occurred even though the current was "on" only 10^{-4} fraction of the test time. Along with the increase in rate, there generally also occurred some change in slip band structure or microstructure. It is proposed that an important factor in the effects produced by the current pulses is the influence of an electron wind on the motion of the atoms and dislocations involved.

The application of a continuous external d.c. electric field of ~ 1 kV/cm **retarded** the following phenomena: (a) recovery and recrystallization of cold worked Al and Cu, (b) grain growth and the formation of cavities during superplastic deformation of the 7475 Al alloy, and (c) quench aging, bainite formation and tempering of steels. The electric field however **increased** the rates of recovery and recrystallization of the superalloy Ni_3Al and the rate of austenization of a tool steel. The effects of the field occurred throughout the bulk of the 1–3 mm thick specimens and not just at the surface, and appear to be associated with the directed atomic mobility produced by a field.

Key Words

Electroplastic, electropulsing, electric field, electric current, electron wind, dislocations, plastic strain rate, recovery, recrystallization, grain growth, fatigue, superplasticity, phase transformations, amorphous alloys, quench aging, hardening, tempering.

A STUDY INTO THE MECHANISM(S) FOR THE ELECTROPLASTIC EFFECT IN METALS AND ITS APPLICATION TO METALWORKING, PROCESSING AND FATIGUE

INTRODUCTION

That electric fields and currents influence atomic mobility has been known for some time [1–4], and is termed **electromigration or electrotransport**. In recent years it is becoming increasingly clear that electric fields and currents can also influence dislocation mobility in crystalline solids [5–14], which is termed **electroplasticity**. Since atomic and dislocation mobility are involved in mechanical properties and phase transformations, it is expected that electric fields and currents will have an effect on these phenomena as well. This has important practical implications regarding: (a) the behavior of materials subjected to an environment which includes electric fields and currents and (b) the development of novel working or processing procedures leading to new microstructures with improved properties. Some technological areas where the effects of electric fields and currents may be especially important are: (a) electromigration in VLSI circuits, (b) power generating and transmission systems, (c) high energy power sources, including electromagnetic propulsion, (d) low and high temperature superconducting devices and (e) working and processing of metals, intermetallic compounds and ceramics. Worthy of mention is that the Soviets have demonstrated that benefits can be obtained by employing high density electric current pulses during the working of metals [15,16] and intermetallic compounds [17].

PRIOR WORK

In view of the potential technological importance of the influence of electric fields and currents on the behavior of metals and alloys, a research program into this subject

was carried out by the author and his coworkers during the period May 1, 1981 to October 31, 1985 under the sponsorship of the U. S. Army Research Office (Grant No. DAAG29–81–K–0075). The results obtained during this period are presented in the final report [18]. Briefly, it was confirmed [11,12] that a high density electric current pulse (~ 10^5 A/cm^2 and ~ 100 μs duration) produced a significant increase in the plastic strain rate (i.e. softening) of metals (Al, Cu, Ni, Fe, Nb, W, Ti) in addition to that resulting from the side effects of the current pulse such as Joule heating and pinch and magnetostrictive effects. The increased strain rate was found to consist of two contributions: (a) an "electron wind" force which is proportional to the current density j and (b) a second, unclear effect which was proportional to j^2. This gave the following expression for the effect of the electric current pulse on the plastic strain rate

$$\dot{\varepsilon}_j/\dot{\varepsilon}_a = \alpha j^2 \exp(\beta j) \qquad \text{(a)}$$

where $\dot{\varepsilon}_j$ is the strain rate occurring during the pulse, $\dot{\varepsilon}_a$ the applied strain rate prior to the application of the pulse and α and β are material constants depending on the test temperature and strain rate. The electron wind force F_{ew} per unit dislocation length was determined for Al and Cu to be

$$F_{ew} = K_{ew} j \qquad \text{(b)}$$

where $K_{ew} \approx 5 \times 10^{-8}$ (dyn/cm)/(A/cm^2).

Regarding metal processing, exploratory studies established that electropulsing (~ 10^5 A/cm^2, ~ 100 μs duration and ~ 2 pulses per s) reduced the force required for drawing Cu wire and enhanced the rates of recovery and recrystallization of cold worked Cu [19] and the rate of sintering of Al powder. Along with the reduction in the recrystallization temperature of Cu produced by the electropulsing there occurred a decrease in the recrystallized grain size and in the annealing twin frequency within

the grains. No detectable effect on the annealing behavior of Cu was noted for a continuous low density current of $10^2 - 10^3$ A/cm^2.

ACCOMPLISHMENTS ON PRESENT GRANT

The work carried out on the present research contract (U. S. ARO DAAL03–86K–0015 for the period November 20, 1985 to November 19, 1988) is a continuation of that mentioned above. The principal objectives of the present program were: (a) to develop further our understanding of the mechanisms responsible for the electroplastic effect in metals and (b) to determine further the effects of electric fields and currents on the mechanical properties of metals (including fatigue and superplasticity) and on solid state transformations (including recrystallization and grain growth, sintering and the quench aging and hardening of steels). The more significant results obtained on this project are presented below.

1. Effects of High-Density Electric Current Pulses

1.1 Theoretical Considerations

Theoretical treatments of the forces exerted by electric fields and currents on point defects (solute or solvent atoms) and line defects (dislocations) in metals and alloys were reviewed in Ref. 20. Briefly, the forces acting on an atom are of two types [2,3,21]: (a) an electrostatic force f_{es} acting on the charged ions and in the direction of the cathode and (b) an electron wind force f_{ew} due to the ballistic impact of the drift electrons acting in the direction of the anode. The electrostatic force is given by

$$f_{es} = -eZE = -Ze\rho j \qquad (1)$$

and the electron wind force by

$$f_{ew} = e\left(\frac{\rho_s}{N_s}\right)\left(\frac{n_e}{\rho}\right)E = e\left(\frac{\rho_s}{N_s}\right)n_e j \qquad (2)$$

where e is the charge on an electron, Z the valence of the atom, E the electric field, ρ the specimen resistivity, j the current density, (ρ_s/N_s) the specific resistivity of the atom and n_e the electron concentration. The total force f_{ea} is the sum of the electrostatic and electron wind forces, giving

$$f_{ea} = e\left(\frac{\rho_s}{N_s}\right) n_e j - Ze\rho j \qquad (3)$$

$$= Z^* e\rho j \qquad (3a)$$

where $Z^* = [Z_o\ (\rho_s/N_s)\ (N/\rho) - Z]$ is an effective valence, whereby Z_o is the valence of the background or host atoms of density N. Considering the Nernst-Einstein equation, it follows that the drift velocity v_a of the atoms is given by

$$v_a = f_{ea} D/kT = Z^* e\rho j D/kT \qquad (4)$$

where D is the appropriate diffusion coefficient and kT has its usual meaning.

Rather good agreement has been obtained between experimental results on electromigration and the predictions of Eq. 4. Typically, Z^* for lattice diffusion in FCC metals is 10 and $\rho = 10^{-6}$ Ω–cm, giving $f_{ea} \approx 10^{-11}$ dyn for $j = 10^6$ A/cm^2. The large positive value for Z^* indicates that f_{ew} is about an order of magnitude larger than f_{es}.

Theoretical treatments of the electron wind force exerted on dislocations are of two types: (a) those based on the specific resistivity of dislocations [22,23] and (b) those based on quantum mechanics and kinetic considerations of the interaction between drift electrons and moving dislocations [24–26]. The former yield for the election wind force per unit dislocation length

$$F_{ew} = e\ (\rho_D/N_D) n_e j \qquad (5)$$

and the latter

$$F_{ew} = \alpha b p_F j/e \qquad (6)$$

where (ρ_D/N_D) is the specific dislocation resistivity, N_D the dislocation density, b the Burgers vector, p_F the Fermi momentum and α = 0.25 to 1.0 depending on the details of the calculation and the exact nature of the Fermi surface. As pointed out by Nabarro [27], Eqs. 5 and 6 are equivalent within a numerical factor of unity, since in the free electron model $bp_F = h$, $j = n_e v_e e$ and $(\rho_D/N_D) = (4h/n_e e^2)$ [28], where h is Plancks constant and v_e the electron drift velocity.

A relationship similar to Eq. 5 was obtained by the author [29] by assuming that the scattering of electrons by a dislocation is approximated by the scattering from a row of point defects. Starting with Eq. 2 above, one then obtains for the electron wind force per unit dislocation length

$$F_{ew} = f_{ew}/b = \frac{1}{b}\left[\rho_D/\left(N_D/b\right)\right] en_e j \qquad (10)$$

$$= e\left(\rho_D/N_D\right) n_e j \qquad (10a)$$

which is identical to Eq. 5. Following the same line of reasoning, we obtain for the electrostatic force per unit dislocation length

$$F_{es} = f_{es}/b = -Ze\rho j/b \qquad (11)$$

and for the total force on a dislocation

$$F_{eD} = Z^{*} e\rho j/b \qquad (12)$$

where $Z^{*} = Z_o b\,(\rho_D/N_D)\,(N/\rho) - Z$. For $j = 10^6$ A/cm^2, Eq. 12 yields ~ 10^{-2} dyn/cm for the common FCC metals. As in the case of point defects, the magnitude of the electron wind force on a dislocation in metals is approximately an order of magnitude greater than the electrostatic force.

Additional parameters of importance in theoretical considerations of the effects of electric fields and currents on dislocations are the electron wind force coefficient K_{ew} =

F_{ew}/j and the electron wind push coefficient $B_{ew} = F_{ew}/v_e = K_{ew}en_e$, where $v_e = j/en_e$ is the electron drift velocity.

The increase in plastic strain rate $\dot{\gamma}$ resulting from an electron wind acting on a dislocation was evaluated [20] for two conditions: (a) when the running time t_r between obstacles to dislocation motion is much longer than the waiting time t_w at the obstacle and (b) when $t_w >> t_r$. For the case when $t_r >> t_w$, one obtains for the ratio of the plastic strain rate with current $\dot{\gamma}_j$ to that without current $\dot{\gamma}_{j=o}$

$$\frac{\dot{\gamma}_j}{\dot{\gamma}_{j=o}} = \frac{B(B\dot{\tau}_a b - B_{ew}^2 v_e)}{\dot{\tau}_a b(B^2 - B_{ew}^2)} \qquad (13)$$

where $B = \tau_a^* b/v_D$ is the electron drag coefficient (v_D is the dislocation velocity), $B_{ew} = F_{ew}/v_e$ the electron push coefficient (v_e is the electron drift velocity) and τ_a^* the effective externally applied stress. For the case when $t_w >> t_r$, one obtains upon employing the model shown in Fig. 1

$$\frac{\dot{\gamma}_j}{\dot{\gamma}_{j=o}} = \frac{\left\{\dot{\gamma}_o \exp -\left[\frac{\Delta G^* - A^* \tau_a^* b}{kT}\right]\right\}_j 2\cosh\left(\frac{A_j^* F_{ew}}{kT}\right)}{\left\{\dot{\gamma}_o \exp -\left[\frac{\Delta G^* - A^* \tau_a^* b}{kT}\right]\right\}_{j=o}} \qquad (14)$$

where $\dot{\gamma}_o = N_{D,m} b \bar{s} \nu^*$ is the pre-exponential factor, $N_{D,m}$ the mobile dislocation density, b the Burgers vector, $\bar{s}$ the average distance moved per successful fluctuation ν^* the frequency of vibration of the dislocation, ΔG^* the Helmholtz free energy of activation and A^* the activation area. The subscript j indicates that the designated parameters may vary with current density.

1.2 Electroplastic Effect – Monotonic Stressing

1.2.1 Measurement of the Electroplastic (ep) Effect: One method for

determining the magnitude of the effect of an electric current on plastic flow (i.e., the electroplastic (ep) effect) is from the drop in flow stress which results upon application of a high density (10^4–10^6 A/cm^2) electric current pulse (~ 100 μs duration) during the tensile straining of a metal [11,12]. Important in such determinations is the elimination of all side effects of the current pulse including: (a) thermal expansion and thermally activated plastic flow resulting from Joule heating, (b) pinch, skin and magnetostrictive effects and (c) load oscillations due to the inertia of test system. Methods and procedures for eliminating these side effects were developed and are presented in Refs. 11–12,30. Employing these, one can then obtain the magnitude of the ep effect, i.e., the increase in plastic strain rate which results from the direct interaction between drift electrons and dislocations.

1.2.2 Magnitude of the Electroplastic Effect-Electron Wind Force: Data from the Soviet literature and those obtained on this research grant for the increase in plastic strain rate $\dot{\varepsilon}$ resulting from the application of a single current pulse during a constant strain rate test at low homologous temperatures ($T < 0.5\ T_m$), or from multi pulses during creep or stress relaxation tests, are presented in Fig. 2. The results indicate that only little, if any, effect occurs for $j < \sim 10^3$ A/cm^2; however, a significant increase in $\dot{\varepsilon}$ occurs at higher current densities, giving

$$\dot{\varepsilon}_j/\dot{\varepsilon}_{j=o} = (j/j_c)^n \qquad (15)$$

where $\dot{\varepsilon}_j$ is the plastic strain rate with current, $\dot{\varepsilon}_{j=o}$ the rate without current, j_c the critical current density and $n \approx 3$. The results for the Zn crystals show that the effect of the current is the same in the three types of testing (flow stress, creep and stress relaxation), and for multi current pulses as for a single pulse. j_c was found to be related to the electron concentration n_e through (see Fig. 3)

$$j_c = cn_e^{2/3} \qquad (16)$$

where $c = 1.5 \times 10^{11}$ A.

Evidence indicating that a significant portion of the increased plastic strain rate resulting from a current pulse is caused by an electron wind force is provided by the observed polarity effects on plastic flow [7,31] and on dislocation velocity [32]. The elegant experiments of Boiko et al [31] are especially noteworthy in this regard.

Values for the electron wind force for a number of metals were determined from the slopes of semilog plots of $\dot{\varepsilon}_j/\dot{\varepsilon}_{j=o}$ vs. A^* (or A^{*2}) [11,12,20], based on the model of Fig. 1 and Eq. 14. The values of F_{ew} so derived were proportional to j and in reasonable accord with the predictions of Eqs. 5, 6 and 10; see Table 1. The intercepts (designated **a**) of the semilog plots (reflecting the effect of the drift electrons on the parameters comprising $\dot{\gamma}_o$, and their effect on ΔG^* and A^*) increased with current density according to

$$a = (j/j_{c,a})^{n^*} \qquad (17)$$

where $j_{c,a} \approx 10^4$ A/cm^2 and $n^* \approx 2$. By combining the two contributions (F_{ew} and **a**) to the ep effect, one obtains

$$\dot{\varepsilon}_j/\dot{\varepsilon}_{j=o} = \alpha j^2 \exp(\beta j) \qquad (18)$$

where α and β are material constants depending on the test temperature and prior strain rate.

A review of the constitutive equations which apply to the electroplastic effect in Cu at low homologous temperatures is given in [33].

1.2.3 Effects of Stacking Fault Energy and Temperature on the Electroplastic Effect in FCC Metals: To further evaluate the ep effect in FCC metals, the influence of stacking fault energy (as manifested by the metals Al, Cu, Ag) and temperature (77 and 300K) on the drop in flow stress resulting from a current pulse were determined

[34]. Fig. 4 shows that the electron wind push coefficient B_{ew} (= F_{ew}/v_e = F_{ew} en_e/j) derived in these experiments increases with decrease in stacking fault energy γ_{SF} and with increase in temperature T, the effect of T however becoming smaller as γ_{SF} increases. The variation of B_{ew} with dislocation splitting width d^* (= $\mu b^2/[12\pi\ (\gamma_{SF} + \tau_a^* b)]$) is presented in Fig. 5. It is here seen that B_{ew} increases with d^*, the effect being greater as T increases. An increase in B_{ew} with T is in keeping with the trend in the specific dislocation resistivity (ρ_D/N_D) with temperature [35].

The effects of γ_{SF} and T on the parameter **a** of Eq. 17 were mainly to cause an increase in the critical current density $j_{c,a}$.

1.2.4 Effect of Strain Rate on the Electroplastic Effect in Nb: Since no previous definitive study had been carried out on the effect of the prior strain rate on the electroplastic effect in metals, the influence of strain rate $\dot{\varepsilon}$ in the range of 1.7×10^{-5} to $8.4 \times 10^{-4} s^{-1}$ on the ep effect in Nb at 300K was determined [36]; see Fig. 6 Here $\Delta\varepsilon_p$ is the measured electroplastic strain and $\Delta\varepsilon_{ed}$ the corrected value taking into account the thermally-activated plastic flow which occurred between completion of the pulse (t ≈ 100 μs) and the measurement of the load drop (t = 60 ms). The ep effect increased with increase in $\dot{\varepsilon}$, in accord with an electron force acting at an increasingly higher level on the force-activation distance curve (i.e., at a lower ΔG^*).

1.3 Electroplastic Effect-Cyclic Stressing

It was determined [37] that the concurrent application of high density electric current pulses (1.3×10^{-4} A/cm^2, ~ 100 μs duration and 2 per s) increased the fatigue life N_f of Cu in rotating bending at 300K by a factor of 1.2 – 3.0; see Fig. 7. The increased fatigue life reflected both an increase in the number of cycles for microcrack initiation and a decrease in macrocrack growth rate. The increase in N_f due to current pulsing is especially significant, since the current was "on" only ~ 10^{-4} fraction of the total test time.

Along with the increase in fatigue life the electropulsing produced a decrease in the persistent slip band (PSB) spacing x (i.e., an increase in linear slip band density n = 1/x), in the PSB width w (Figs. 8 and 9), and apparently in the dislocation density determined by TEM. Microcrack initiation occurred only along the PSBs (transgranular) at the lowest stress (high cycle fatigue) and mostly along grain boundaries (intergranular) at the higher stresses (low cycle fatigue). Electropulsing increased the tendency for transgranular compared to intergranular cracking. The fatigue life (cycles to fracture N_f) at all stress levels was proportional to the ratio n_f/w_f, in accord with an initial crack depth criterion for fatigue life at low stresses [38] and a PSB-grain boundary interaction model at the higher stresses [37]. The increase in microcrack initiation life resulting from the electropulsing was attributed to the increased homogenization of slip produced by the current pulses.

SEM observations of the fracture surfaces of the fatigued specimens revealed an increased oxidation due to electropulsing. The observed decrease in macrocrack growth rate produced by the electropulsing was therefore attributed to a decrease in ΔK_{eff} resulting from the presence of the thicker oxide film and its influence on crack closure.

1.4 Annealing

Electropulsing (~ 10^5 A/cm^2, ~ 100 μs duration and 2 per s) applied during the annealing of Cu [19,39,40] enhanced the rates of recovery and recrystallization (Fig. 10), and retarded the rate of grain growth (Fig. 11). Also, there occurred a finer recrystallized grain size, a reduced annealing twin frequency and a sharper [112] texture [40]. The degree of enhancement of the recrystallization rate decreased as the amount of prior cold work increased [19]. The current pulsing enhanced the recrystallization kinetics through the pre-exponential factor, having essentially no effect on the activation energy [39]. Again, the effects of electropulsing are especially

remarkable, since the maximum temperature rise from Joule heating was only 2°C and the current was on only about 10^{-4} **fraction** of the total annealing time.

The effect of current pulsing on recrystallization is attributed to its influence on the rate of subgrain formation and coalescence; its effect on grain growth to the increased rate of annihilation of residual dislocations, which provided the major driving force for grain growth at the test conditions considered. Only a small increase in the annealing twin frequency resulted from the electropulsing when the effect of grain size on twinning was taken into account [40]. The effect of current pulsing on texture indicates an influence on recrystallized grain nuclei orientation and/or preferred growth direction.

Enhanced rates of recovery and recrystallization were also found to occur when current pulsing was applied during the annealing of high purity (99.996%) and commercial purity (99+%) Al (Fig. 12), and the intermetallic compound Ni_3Al containing boron (Fig. 13).

1.5 Phase Transformations

1.5.1 Crystallization of Iron-Based Amorphous Alloys: Electropulsing (~ 10^5 A/cm^2, 60–95 μs duration and 4.2 to 8.7 pulses per s) led to α-Fe precipitation in two amorphous iron-based alloys ($Fe_{75}Si_{10}B_{15}$ and $Fe_{79}Si_7B_{14}$) at temperatures well below (~ 150°C below) those where bulk crystallization first occurred without an electric current [41]. The enhanced rate of precipitation could result from an increased diffusion rate (electromigration) produced by action of the current.

1.5.2 Crystallization of an Amorphous TiCu Alloy: The effect of current pulsing on a rapidly quenched, amorphous TiCu alloy (obtained from Prof. T. Massalski of Carnegie Mellon University) was investigated to determine whether transformation to a crystalline form could be induced below the glass transition temperature T_g = 573K in this alloy. No transformation was detected by x-ray diffraction for the following

electropulsing conditions: $j = 1.14 \times 10^5$ to 1.52×10^5 A/cm^2, $t_p = 100 - 300$ μs, $\nu_p = 2$ pulses per s, total time of heating t = 8 hr and temperature T = 387 – 488K.

1.5.3 Tempering of Steel: Limited tests indicated that a **continuous** d.c. current of 6.5×10^2 A/cm^2 enhanced the tempering rate of a 0.9 C tool steel only slightly, an equivalent 60 Hz a.c. current had still less effect, as did also a pulsed d.c. current of 5.85×10^4 A/cm^2, 100 μs duration and 2 pulses per s (equivalent continuous d.c. current of ~ 6 A/cm^2); see Fig. 14.

1.6 Sintering

The porosity of cold pressed (uniaxial and hydrostatic) Al powder compacts (3 x 3 x 6 mm) was reduced ~ 30% by sintering at room temperature for 30 min employing the following electropulsing conditions: $j = 2.7 \times 10^5$ A/cm^2, $t_p = 10$ μs and 1 pulse per 30 s.

2. Effects of a Continuous External D.C. Electric Field

2.1 Superplasticity

The application of a continuous external d.c. electric field E of ~ 2 kV/cm to a 7475 Al alloy specimen undergoing superplastic deformation in tension at 520°C produced the following effects [42]: (a) a decrease in the flow stress, i.e. a lowered stress-strain curve, (b) a decrease in the strain hardening rate $d\sigma/d\varepsilon$ (Fig. 15), (c) a slight increase in the strain rate hardening exponent $m = d\ln\sigma/d\ln\dot{\varepsilon}$ (Fig. 16) and (d) an approximately four-fold reduction in the volume fraction of cavities **throughout the bulk of the 1.2 mm thick specimen (Fig. 17).** The experimental arrangement consisted of making the specimen one electrode of a capacitor with air as the dielectric medium. The exact mechanism(s) by which these effects occur are not clear at this time, especially since the electric field within the bulk of the alloy is expected to be essentially zero (the current flow was only of the order of a mA). It appears that the action of the electric field at the surface influences behavior in the bulk as well.

2.2 Annealing

The application of an electric field of 2.4 – 8.0 kV/cm during the isochronal annealing of Cu and Al produced an increase in the recovery and recrystallization temperatures (Figs. 18 and 19) [42], indicating that the field retarded these phenomena. This effect is opposite to that for electropulsing, which enhanced their rates [19,39,40]. Further, as is evident in Fig. 18, the effect of the field increased with increase in amount of prior cold work. Again, this is opposite to what was found for electropulsing [19]. Also, worthy of note in Fig. 18 is that no difference in the influence of the electric field occurred for the range of 2.4 to 8.0 kV/cm, nor by changing the environment with dielectric constants varying from 1.0 to 2.5. **Again, the effects of the electric field occurred throughout the bulk of the 1 mm dia. specimen, not just at the surface.**

2.3 Phase Transformations

2.3.1 Quench Aging of Iron: Exploratory studies indicate that an electric field of 10 kV/cm retards quench aging in a 99.9% iron; see Fig. 20.

2.3.2 Quench Hardening and Tempering of Steel: Exploratory studies [44] revealed that an electric field of 1–2 kV/cm applied during quench hardening and tempering of a 4340 steel and a 02 (0.9 C) tool steel produced the following effects: (a) an increase in the rate of austenizing (Fig. 21), (b) an increase in hardenability (Fig. 22) and (c) a slight retardation of the tempering rate (Fig. 23). Limited optical microscopy and TEM observations on the 4340 steel quenched in mineral oil revealed the following effects of the electric field on the microstructure: (a) a slight reduction in the austenite grain size, (b) a reduction in the amount of upper bainite and (c) a reduction in the density of microtwins in the martensite. **Again, the effects of the electric field occurred throughout the bulk of the 2–3 mm dia. specimen**

and not just at the surface. It is proposed that directed diffusion produced by the field may be a factor in the observed effects.

3. Relevant Research Activities

3.1 Electromigration

The Bloch-Kinsborn technique [45,46] was employed to determine the effect of an externally applied stress on the atomic drift velocity in an Al film vapor deposited on a Si wafer. It was found that the drift velocity at 200°C and $j = 10^6$ A/cm^2 increased by a factor of 3.6 upon application of a compressive stress of 25 MPa compared to zero stress, Fig. 24. This effect of stress is in keeping with the chemical potential gradient established by the electron wind assisted atomic movements towards the anode junction [45,46].

3.2 Plastic Instability

The plastic deformation parameters which govern **local** necking in 3003–0 Al sheet at 300K were defined and evaluated in terms of dislocation behavior [47]. To this end, the dislocation density as a function of strain was determined by four methods: (a) from Bergstrom's model applied to the true stress-strain curve, (b) from strain rate cycling tests, (c) x-ray diffraction and (d) TEM. Good agreement was obtained between the four methods. The plastic deformation parameters were considered in terms of: (a) intersection of dislocations, (b) long-range internal stress due to dislocations and (c) dislocation multiplication rate. The variation of the effective flow stress $\bar{\sigma}$ with total dislocation density ρ from yielding through local necking was given by

$$\frac{\bar{\sigma}}{M} = 0.33\,\mu b \rho^{1/2}$$

where M (= 3.1) is the Taylor orientation factor, μ the appropriate shear modulus and b the Burgers vector.

3.3 Dislocation Structure and Dynamics

A two-parameter representation of the dislocation segment length distribution is proposed to represent the plastically deformed state of a material [48]. This distribution function represents the radii to which dislocations are bowed during plastic deformation. It is based on the premise that both a minimum and a maximum value of radius exists. Various quantities associated with the plastically deformed state, namely the fraction of mobile dislocations, the stress dependence of strain rate and of the dislocation velocity are derived from the two-parameter distribution function. The distribution function is also applied to the plastic deformation behavior of polycrystalline copper in tension, in torsion and in tension plus torsion. The results illustrate that the two-parameter distribution explains different characteristic features of plastic deformation and also distinguishes the different forms of plastic deformation of solids.

ACKNOWLEDGEMENTS

The author acknowledge the invaluable assistance of Dr. A. F. Sprecher, senior research associate, in carrying out all phases of this research program. Also, Dr. K. Bae, Ms. X. P. Lu and Mr. Z. Guo contributed substantially to the research work. Further, the author wishes to recognize the following graduate students, who participated in this research project:

Wei-di Cao

M. Fisher

P. Hacke

A. Srivatsa

K. Wade

J. White

A. Zayed

REFERENCES

1. M. Geradin, Comp. Rend. **53** (1961) 727.

2. H. B. Huntington, in **Diffusion**, ASM, Metals Park, OH (1973) 155.

3. **Electro- and Thermo-transport in Metals and Alloys**, ed. by R. E. Hummel and H. B. Huntington, AIME, NY (1977).

4. F. D'Heurle and P. S. Ho, in **Thin Films-Interdiffusion and Reactions**, ed. by J. M. Poate, K. N. Tu and J. W. Mayer, Wiley-Interscience, NY (1978) 243.

5. O. A. Troitskii, Zh. ETF Piz. Red. **10** (1969) 18.

6. O. A. Troitskii and A. G. Rozno, Fizika Tverdogo Tela **12** (1970) 161.

7. O. A. Troitskii, Prob. Prochnosti No. 7 (1975) 14.

8. O. A. Troitskii, Dokl. Adkad. Nauk SSSR **220** (1975) 1070.

9. K. Okazaki, M. Kagawa and H. Conrad, Scripta Met. **12** (1978) 1063; **13** (1979) 277; **13** (1979) 473.

10. K. Okazaki, M. Kagawa and H. Conrad, Mat. Sci. Engr. **45** (1980) 109; in **Titanium 80 Science and Technology**, TMS-AIME (1980) 763.

11. H. Conrad, A. F. Sprecher and S. L. Mannan, in **The Mechanics of Dislocations**, ASM (1985) 225.

12. A. F. Sprecher, S. L. Mannan and H. Conrad, Acta Metall. **34** (1986) 1145.

13. L. Colombo, T. Kataoka and J. C. M. Li, Phil. Mag. **A46** (1982) 211; **A49** (1984) 395, 409.

14. J. C. M. Li, in **The Mechanics of Dislocations**, ASM (1985) 85.

15. O. A. Troitskii, V. I. Spitsyn, N. V. Sokolov and V. G. Ryzhkov, phs. stat. sol. (a) **52** (1979) 85.

16. O. A. Troitskii, Mat. Sci. Engr. **75** (1985) 37.

17. K. M. Klimov, A. M. Mordukhovich, A. M. Glezer and b. V. Molotilov, Russian Metall. No. 6 (1981) 68.

18. H. Conrad, "A Study into the Mechanism(s) for the Electroplastic Effect in Metals and Its Application to Metalworking", Final Report ARO Proposal No. 18184–MS, Res. Agreement No. DAAG–29–81–K–0075, Dec. 31, 1985.

19. H. Conrad, N. Karam and S. Mannan, Scripta Met. **17** (1983) 411; **18** (1984) 275.

20. H. Conrad and A. F. Sprecher, "The Electroplastic Effect in Metals", in **Dislocations in Solids**, ed. by F. R. N. Nabarro, Elsevier Science (1989) in print.

21. R. S. Sorbello, **Electro- and Thermo-transport in Metals and Alloys**, ed. by R. E. Hummel and H. B. Huntington, AIME, N.Y. (1977) p. 2.

22. F. R. N. Nabarro, **Theory of Dislocations**, Clarendon Press, Oxford (1967) p. 529.

23. A. M. Roshchupkin, V. E. Miloshanko and V. E. Kalimin, Fiz. Tverd, Tela (Leaningrad) **21** 909 (1978).

24. V. Ya. Kravchenko, Zh. Eskp. Theor. Fiz. **51** 1676 (1966).

25. M. I. Kaganov, V. Ya. Kravchenko and V. D. Natskik, Usp. Fiz. Nauk **111** 655 (1973).

26. K. M. Klimov, G. O. Shnyrev and I. I. Movikov, Dolk. Akad. Nauk S.S.S.R. **219** (2) 323 (1974).

27. F. R. N. Nabarro, private communication (1988).

28. R. A. Brown, J. Phys. F: Metal Phys. **7** 1269, 1283 (1977).

29. H. Conrad, reported in Ref. 20.

30. W. D. Cao, A. F. Sprecher and H. Conrad, "Measurement of the Electroplastic Effect in Nb", submitted to J. Physics E: Scientific Instruments (1988).

31. Yu I. Boiko, Ya E. Geguzin and Yu. I. Klinchik, Zh. Eskp. Theor. Fiz. **30** 168 (1979); **81** 2175 (1981).

32. L. B. Zuev, V. E. Gromov, V. F. Kurilov and L. I. Gurevich, Dokl. Akad. SSSR **239** 84 (1978).

33. H. Conrad, Wei-di Cao and A. F. Sprecher, "Constitutive Laws Pertaining to Electroplasticity in Metals", accepted for publ. **19th Canadian Fracture Conf.**, Univ. Ottawa, 29–31 May, 1989.

34. W. Cao, A. F. Sprecher and H. Conrad, "Effects of Stacking Fault Energy and Temperature on the Electroplastic Effect in FCC Metals", in preparation for submission to Phil. Mag.

35. V. F. Gantmakher and G. I. Kulasko, Zh. Eksp. Theor. Fiz. **67** 2335 (1974).

36. W. Cao, A. F. Sprecher and H. Conrad, "The Effect of Strain Rate on the Electroplastic Effect in Nb", Scripta Met. **23** (1989) 151

37. H. Conrad, J. White, A. F. Sprecher, Wei-di Cao and X. P. Lu, "Effect of High Density Electric Current Pulses on the Fatigue of Cu", submitted to Mat. Sci. Engr.

38. W. Cao, A. F. Sprecher and H. Conrad, "Correlation of Fatigue Life with Persistent Slip Band Parameters", submitted to Acta Met.

39. H. Conrad, N. Karam, S. Mannan and A. F. Sprecher, Scripta Met. **22** 235 (1988).

40. H. Conrad, A. F. Sprecher, W. Cao and X. Lu, **Homogenization and Annealing of Al and Cu Alloys**, ed. by H. Merchant, J. Crane and E. Chia, TMS (1988) p. 227.

41. Z. H. Lui, H. Conrad, Y. S. Chao, S. Q. Wang and J. Sun, "Effect of Electropulsing on the Microstructure and Properties of Iron-Based Amorphous Alloys", Scripta Metall, in print.

42. H. Conrad, W. Cao, X. Lu and A. F. Sprecher, "Effect of an Electric Field on the Superplasticity of 7475 Al", to be publ. Scripta Met.

43. H. Conrad, Z. Guo and A. Sprecher, "Effect of an Electric Field on the Recovery and Recrystallization of Al and Cu", to be publ. Scripta Met.

44. W. D. Cao, X. P. Lu, A. F. Sprecher and H. Conrad, "Effects of An External Electric Field on the Heat Treatment Response of Steels", submitted to Met. Trans. A.

45. I. A. Blech and E. Kinsborn, Thin Solid Films **25** 327 (1975).

46. I. A. Blech, J. Appl. Phys. **47** 1203 (1976); J. Appl. Phys. **48** 2648 (1977).

47. A. Zayed, Y. Shin and H. Conrad, **Aluminum Alloys: Their Physical and Mechanical Properties**, Vol. III, EMAS, Warley, UK (1986) 1691.

48. K. Jagannandham and H. Conrad, "A Two-Parameter Representation of Dynamic Dislocation Distributions", **2nd Int. Conf. Low-Energy Dislocation Structures**, Univ. of Virginia, Aug. 13–17, 1989, accepted for publ.

TABLE 1. Comparison of measured electron wind push coefficient $B_{ew} = F_{ew}/v_e$ with theoretical values[1]. Units of B_{ew} are in 10^{-4} dyn-s/cm^2 and $K_{ew} = F_{ew}/j$ are in 10^{-8} (dyn/cm)/A/cm^2.

	Theoretical		Experimental				
Metal	$B_{ew} = (\rho_D/N_D)(en_e)^{2(2)}$	$B_{ew} = bp_F n_e$	$K_{ew} = F_{ew}/j$	$B_{ew} = F_{ew}en_e/j$	T(K)	Ref.	Measurement
Al	1.8–15.1	2.3–9.5	2.4	2.4–6.8	298	12	Flow stress of polycrystals
			3.6	3.5–10.2	298	34	Flow stress of polycrystals
Cu	2.3–2.8	3.0–5.2	7.5	9.9–11.0	298	12	Flow stress of polycrystals
			5.4	7.1–7.8	298	34	Flow stress of polycrystals
			1.7–1.9	2.3–2.5	298	31	Effect of polarity on contact area
Ag	1.7	1.3–1.4	7.4	6.9	298	34	Flow stress of polycrystals
Au	1.7	1.3–1.6	1.8	1.9	298	31	Effect of polarity on contact area
W	0.4–12	0.4	4.0	2.6	298	31	Effect of polarity on contact area
Zn	0.1–109	0.4–12.5	141–613	10–296	78	32	$\{11\bar{2}2\}$ <$11\bar{2}3$> dislocation velocity

Notes:

1. Electronic properties taken from Ref. 20.
2. (ρ_D/N_D) values are calculated values from R. A. Brown, J. Phys. Metal Phys. 7 1283 (1977).

Appendix: Scientific Papers, Patent Disclosures and Graduate Student Theses

Scientific Papers

I. Effects of Electropulsing

A. Mechanical Properties

1. A. F. Sprecher, S. L. Mannan and H. Conrad, "On the Mechanisms for the Electroplastic Effect in Metals", Acta Metall. **34** (1986) 1145–1162.

2. H. Conrad and A. F. Sprecher, "The Electroplastic Effect in Metals", in **Dislocations in Solids**, ed. by F. R. N. Nabarro, Elsevier Science, in print.

3. Wei-di Cao, A. F. Sprecher and H. Conrad, "Effect of Strain Rate on the Electroplastic Effect in Nb", Scripta Met. **23** (1989) 151–155.

4. Wei-di Cao, A. F. Sprecher and H. Conrad, "Measurement of the Electroplastic Effect in Nb", submitted to J. Physics E: Scientific Instruments.

5. H. Conrad, Wei-di Cao and A. F. Sprecher, "Constitutive Laws Pertaining to Electroplasticity in Metals", accepted for publ. **19th Canadian Fracture Conf.**, Univ. Ottawa, 29–31, May 1989.

6. Wei-di Cao, A. F. Sprecher and H. Conrad, "Correlation of Fatigue Life with Persistent Slip Band Parameters", submitted to Acta Metall.

7. H. Conrad, J. White, A. F. Sprecher, Wei-di Cao and X. P. Lu, "Effect of High Density Electric Current Pulses on the Fatigue of Cu, submitted to Mat. Sci. Engr.

B. Annealing

1. H. Conrad, N. Karam, S. Mannan and A. F. Sprecher, "Effect of Electric Current Pulses on the Recrystallization Kinetics of Copper", Scripta Met. **22** (1988) 235–238.

2. H. Conrad, A. F. Sprecher, Wei-di Cao and X. P. Lu, "Effects of High Density Electric Current Pulses on the Annealing of Copper", in **Homogenization and Annealing of Aluminum and Copper Alloys**, eds. H. D. Merchant, J. Crane and E. H. Chia, TMS (1988) 227–239.

C. *Phase Transformations*

1. Z. H. Lai, H. Conrad, Y. S. Chao, S. Q. Wang and J. Sun, "Effect of Electropulsing on the Microstructure and Properties of Iron-Based Amorphous Alloys", Scripta Met., **23** (1989) 305.

II. Effects of an External Electric Field

A. *Mechanical Properties*

1. H. Conrad, W. D. Cao, X. P. Lu and A. F. Sprecher, "Effect of an Electric Field on the Superplasticity of 7475 Al", Scripta Met., in print.

B. *Annealing*

1. H. Conrad, Z. Guo and A. F. Sprecher, "Effect of an Electric Field on the Recovery and Recrystallization of Al and Cu", Scripta Met, accepted for publ.

C. *Phase Transformations*

1. W. D. Cao, X. P. Lu, A. F. Sprecher and H. Conrad, "Effects of an External Electric Field on the Heat Treatment Response of Steels", submitted to Met. Trans. A.

III. Related Research

1. A. Zayed, Y. Shin and H. Conrad, "Dislocation Mechanisms Operative During Plastic Instability of 3003–0 Al Sheet at 300K", **Aluminum Alloys, Their Physical and Mechanical Properties**, Vol. III, EMAS, Warley, U. K. (1986) 1691–1708.

2. A. Zayed and H. Conrad, "Evaluation of the Parameters Which Govern Local Necking in 3003–0 Al Sheet Tested in Uniaxial Tension at 300K", submitted to Met. Trans A.

3. K. Jagannadham and H. Conrad, "A Two-Parameter Representation of Dynamic Dislocation Distributions", accepted for publ., **2nd Int. Conf. Low-Energy Dislocation Structures**, Univ. VA, Aug. 13–17, 1989,

PATENT DISCLOSURES

1. H. Conrad, A. F. Sprecher and Wei-di Cao, "Process for Improved Superplastic Forming of Metals", submitted to NCSU Patent Office, signed Dec. 18, 1987.

2. H. Conrad and A. F. Sprecher, "Process for Controlling the Rates of Recovery, Recrystallization and Grain Growth in Metals", submitted to NCSU Patent Office, signed Dec. 21, 1987.

3. H. Conrad, A. F. Sprecher and Wei-di Cao, "Process for Increasing the Hardenability of Steel", submitted NCSU Patent Office, signed Nov. 22–23, 1988.

STUDENT THESES

A. M.S.

1. James B. White, "The Effect of Electrical Current on Metal Fatigue", M.S., NCSU (1987).

B. Ph.D.

1. Wei-di Cao, "Effects of Electric Fields and Currents on Metal Properties", Ph.D., NCSU, in preparation, expected (1989).

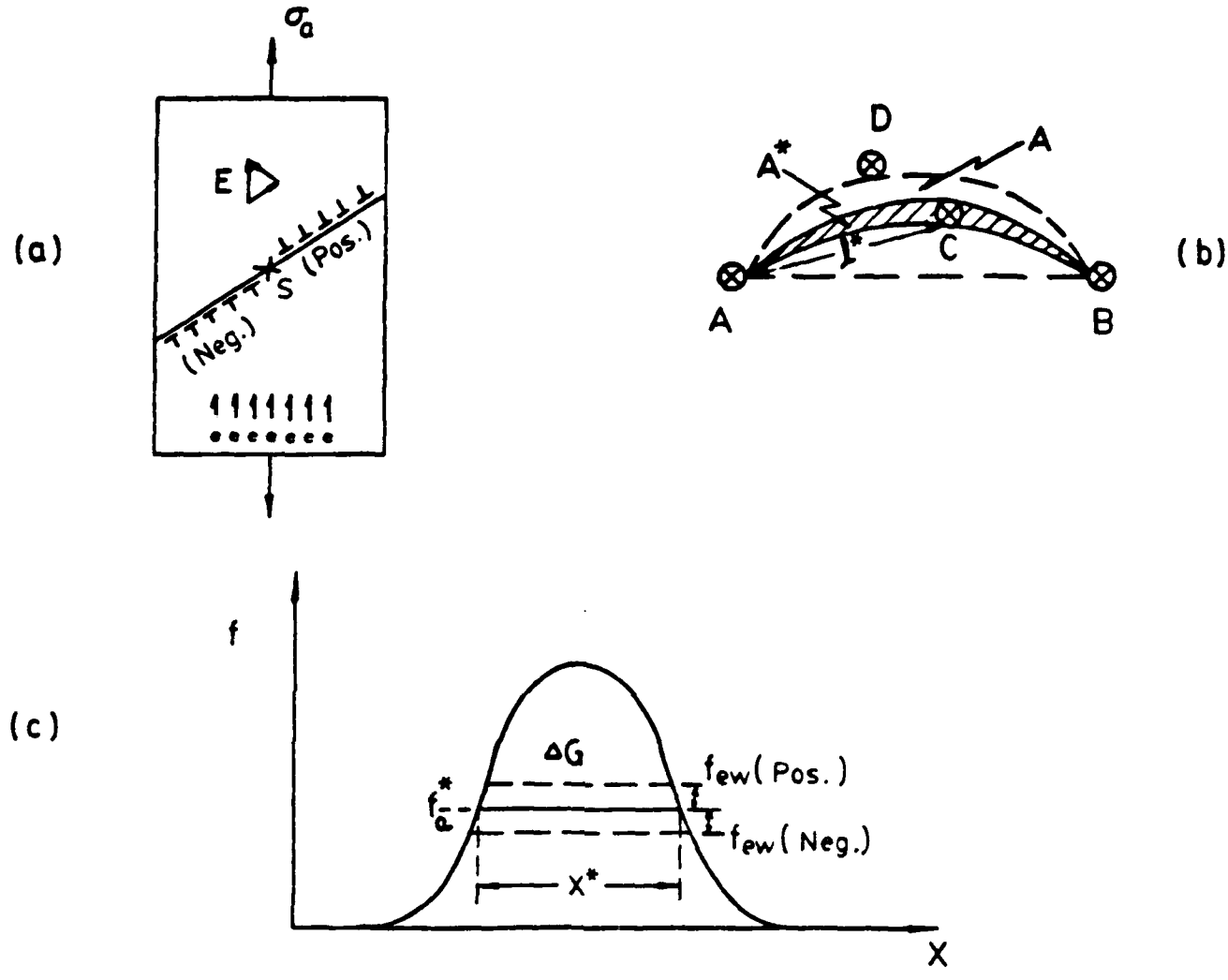

Fig. 1. Schematic pertaining to the effect of an electric field and current on dislocation velocity. (a) Specimen subjected to the combined action of a mechanical stress σ_a and an electric field with dislocations moving on the glide plane with a velocity parallel (pos.) and antiparallel (neg.) to the drift electrons e. (b) Dislocation segment of length $2l^*$ overcomes obstacle C by combined action of total applied force and thermal fluctuations. (c) Force-distance curve for overcoming the obstacle C. ΔG = Gibbs free energy of activation, $f_a^* = \tau_a^* b l^*$, $f_{ew} = F_{ew} l^*$, x^* = activation distance, $A^* = l^* x^*$, $\tau^* = (\sigma_a - \sigma_i)/M$, where σ_i is the long-range internal stress and M the Taylor orientation factor. From Conrad and Sprecher [20].

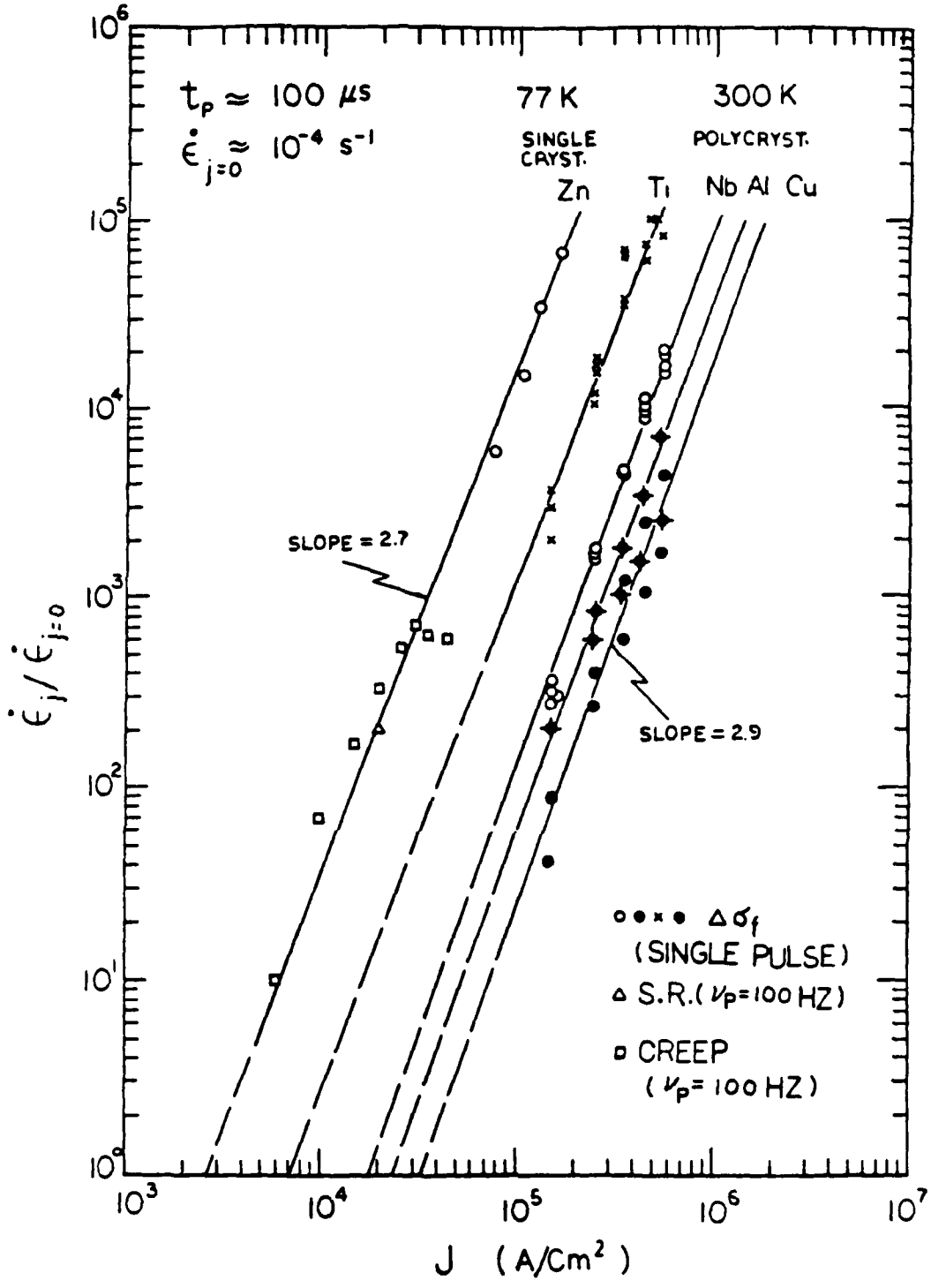

Fig. 2. Log-log plot of $\dot{\epsilon}_j/\dot{\epsilon}_{j=0}$ vs j for Zn single crystals at 78K and a number of polycrystalline metals at 300K. From Conrad and Sprecher [20].

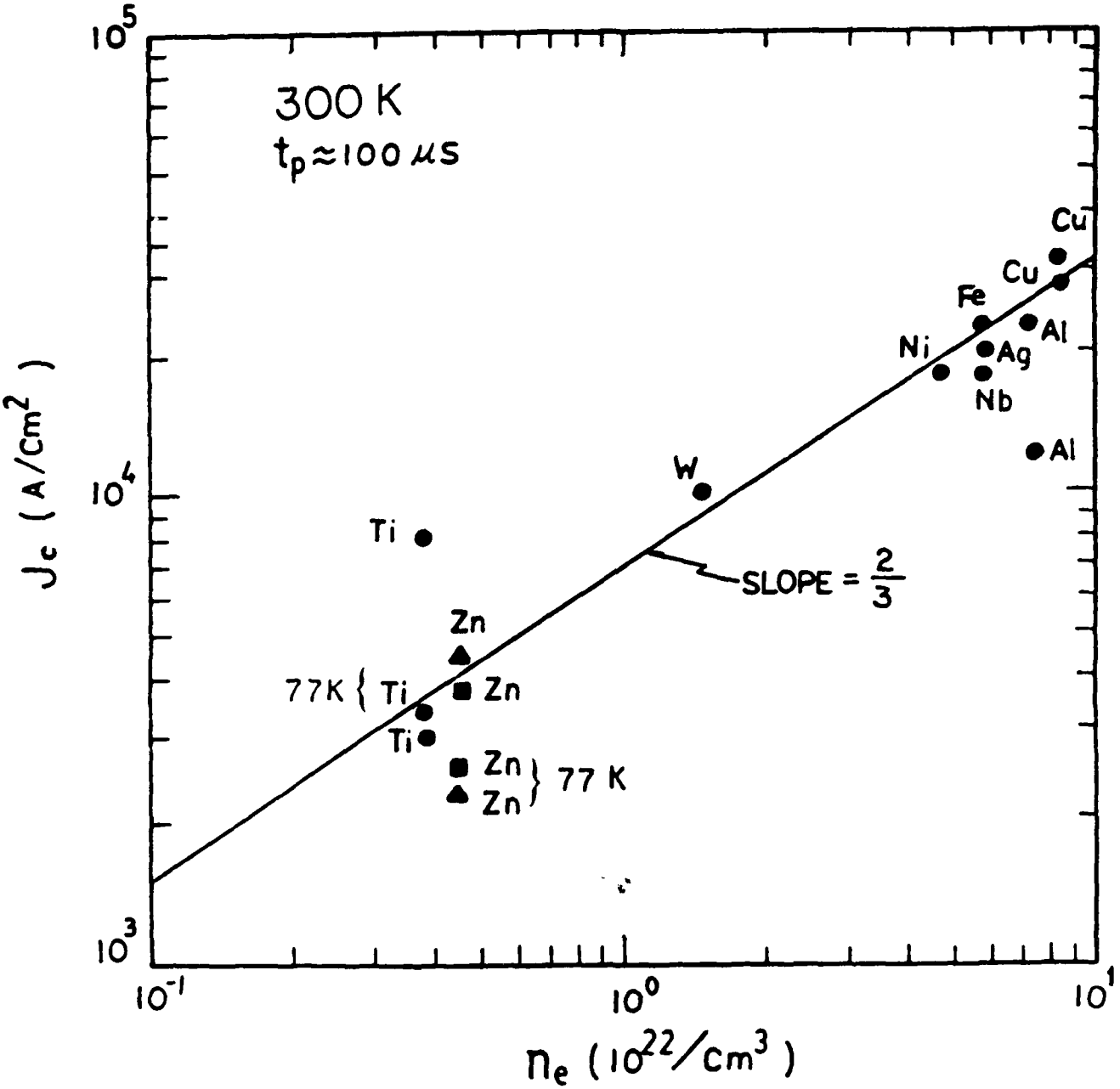

Fig. 3. Log-log plot of j_c vs n_e for the electroplastic effect. From Conrad and Sprecher [20].

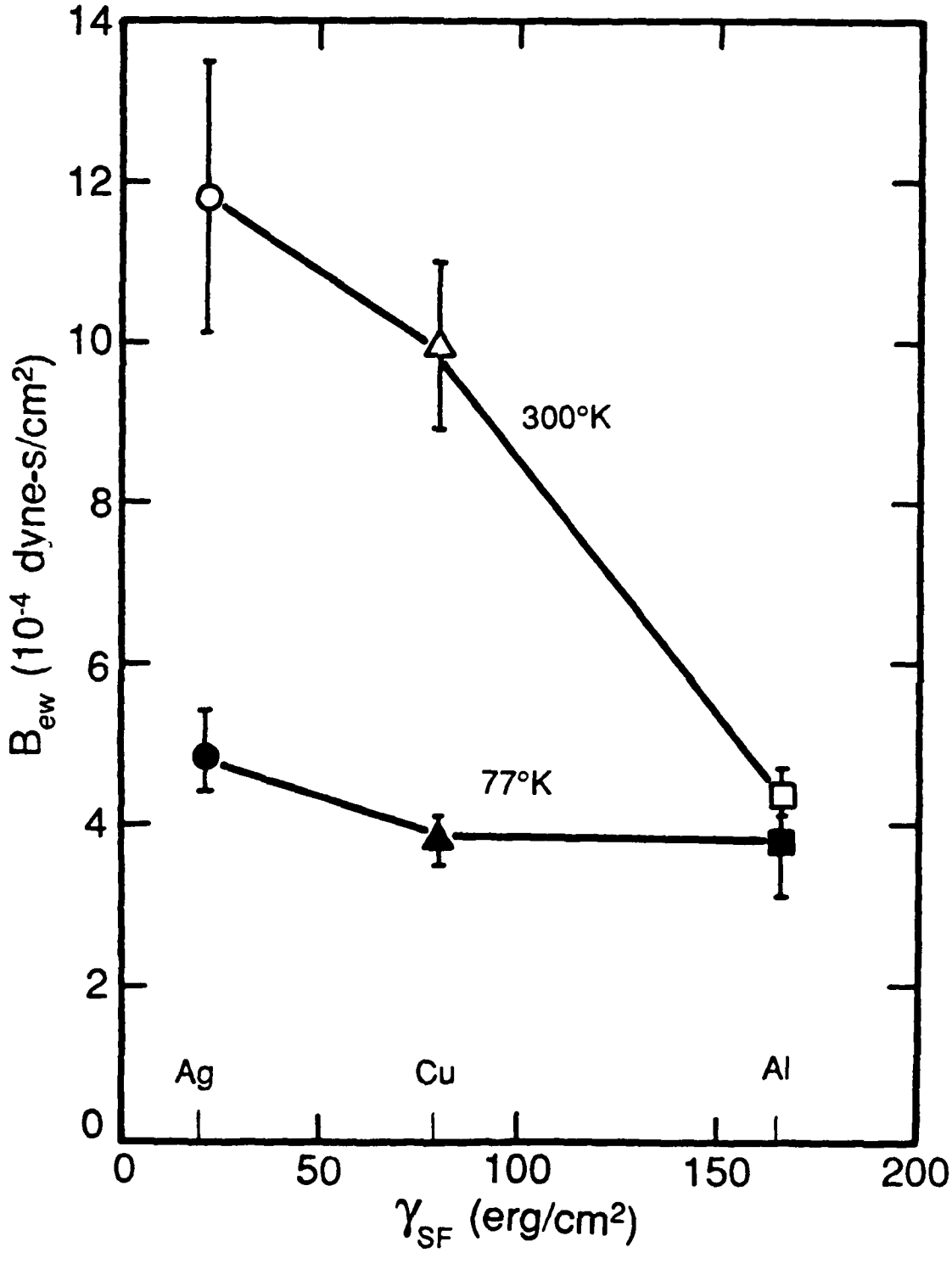

Fig. 4. Effects of stacking fault energy in FCC metals on the electron wind push coefficient B_{ew} as a function of temperature. From Cao, Sprecher and Conrad [34].

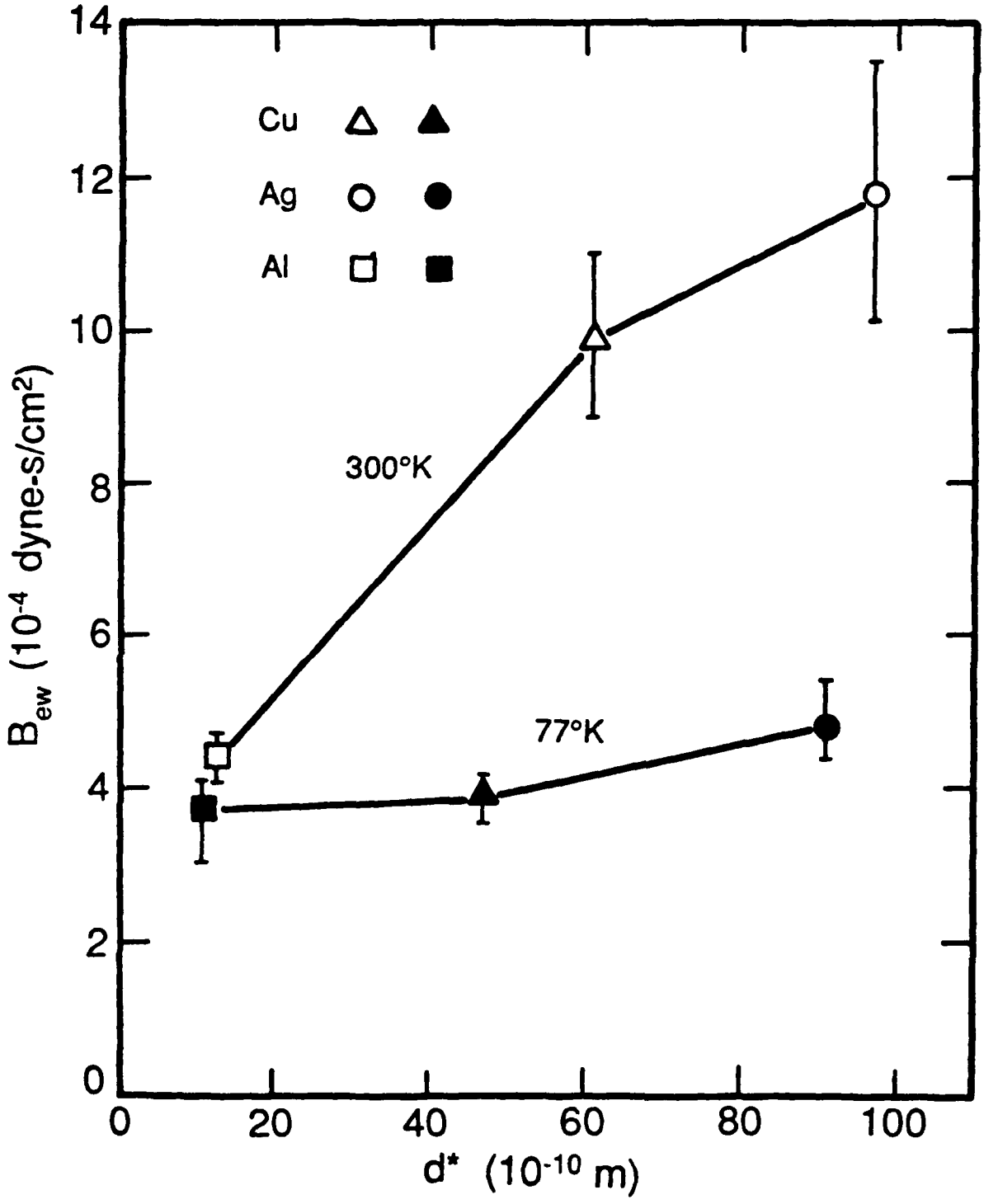

Fig. 5. B_{ew} vs the dislocation splitting width d* in Cu, Ag and Al. From Cao, Sprecher and Conrad [34].

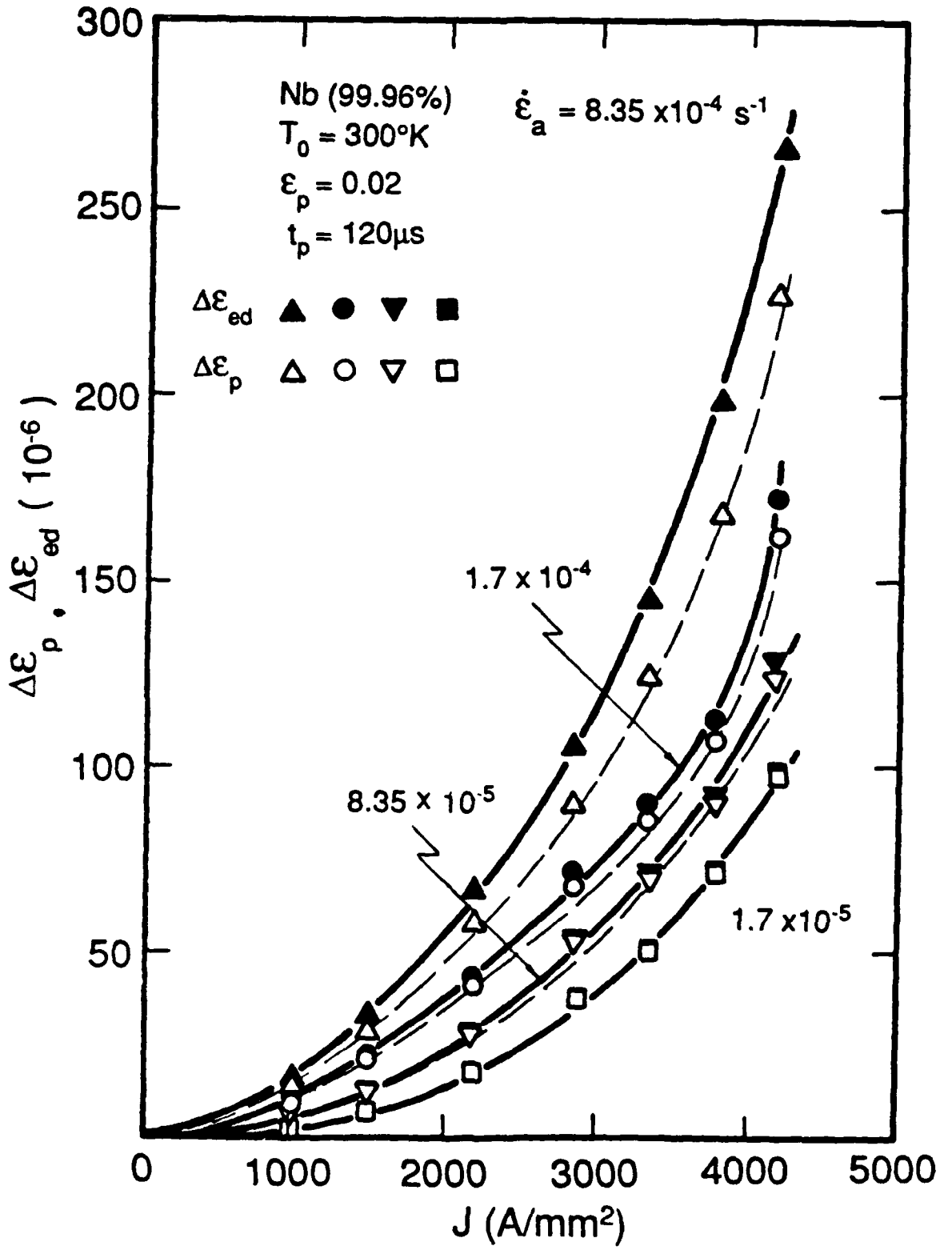

Fig. 6. The corrected electroplastic strain $\Delta\varepsilon_{ed}$ vs current density as a function of prior strain rate in Nb. $\Delta\varepsilon_p$ is the uncorrected electroplastic strain. From Cao, Sprecher and Conrad [36].

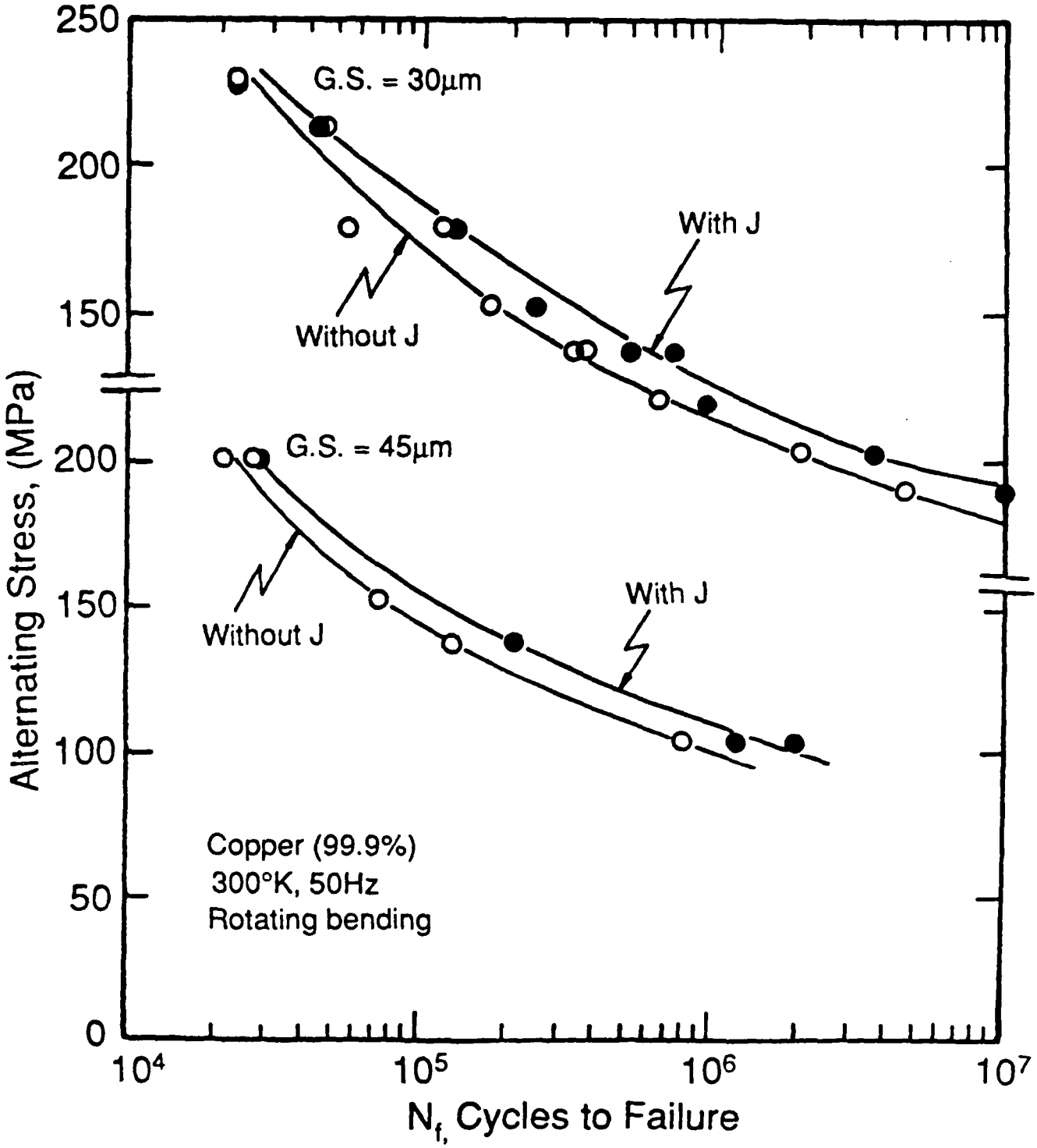

Fig. 7. Effect of electropulsing ($j = 1.3 \times 10^4$ A/cm^2, $t_p = 100$ μs, and $\nu_p = 2$ Hz) on the S-N_4 fatigue behavior of Cu with 30 μm and 45 μm grain size. From Conrad et al [37].

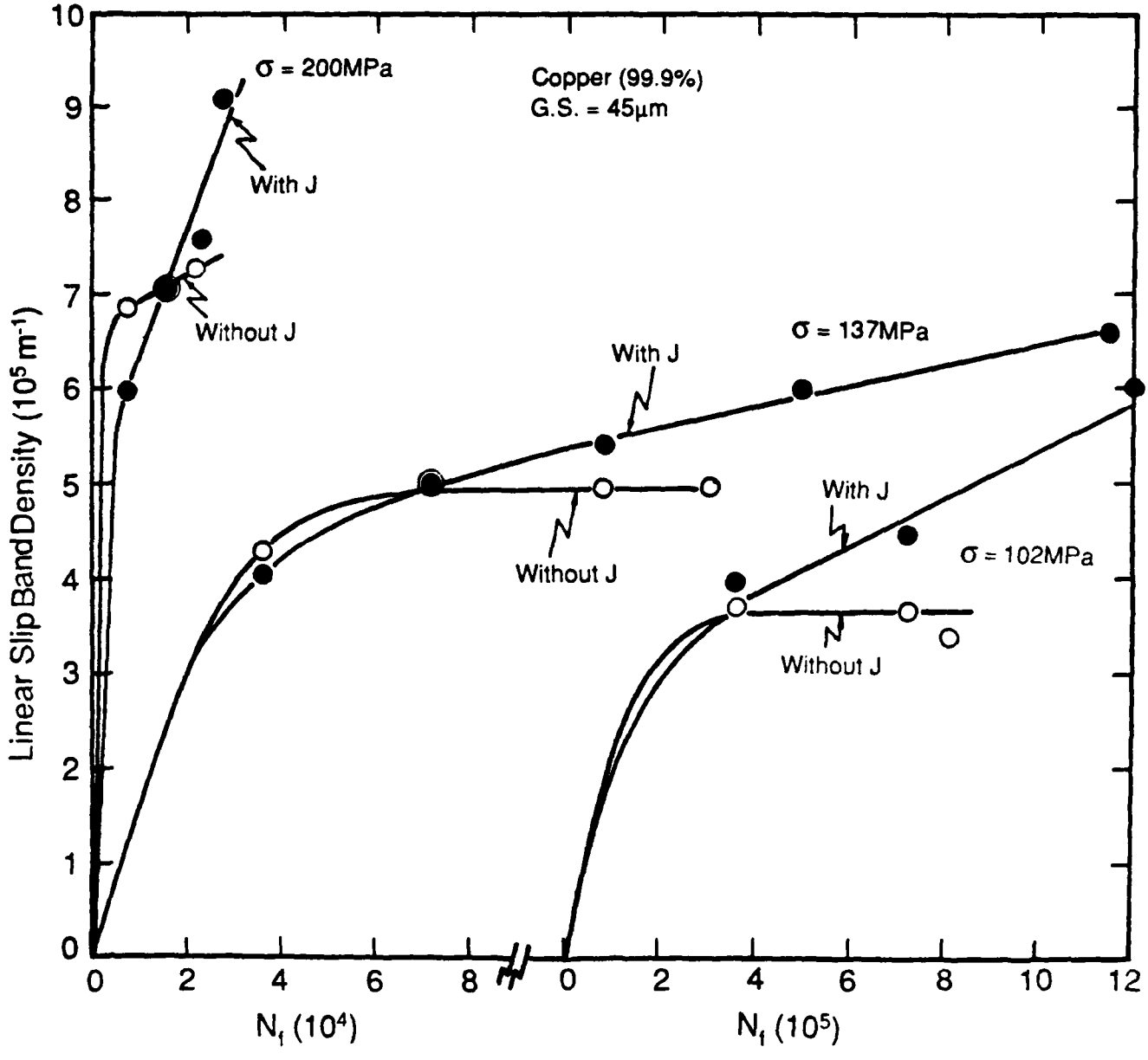

Fig. 8. Effect of electropulsing (j = 1.3 x 10^4 A/cm^2, t_p = 100 μs, v_p = 2 Hz) on the linear PSB density vs number of cycles during the fatigue of Cu in rotating bending at 300K. From Conrad et al [37].

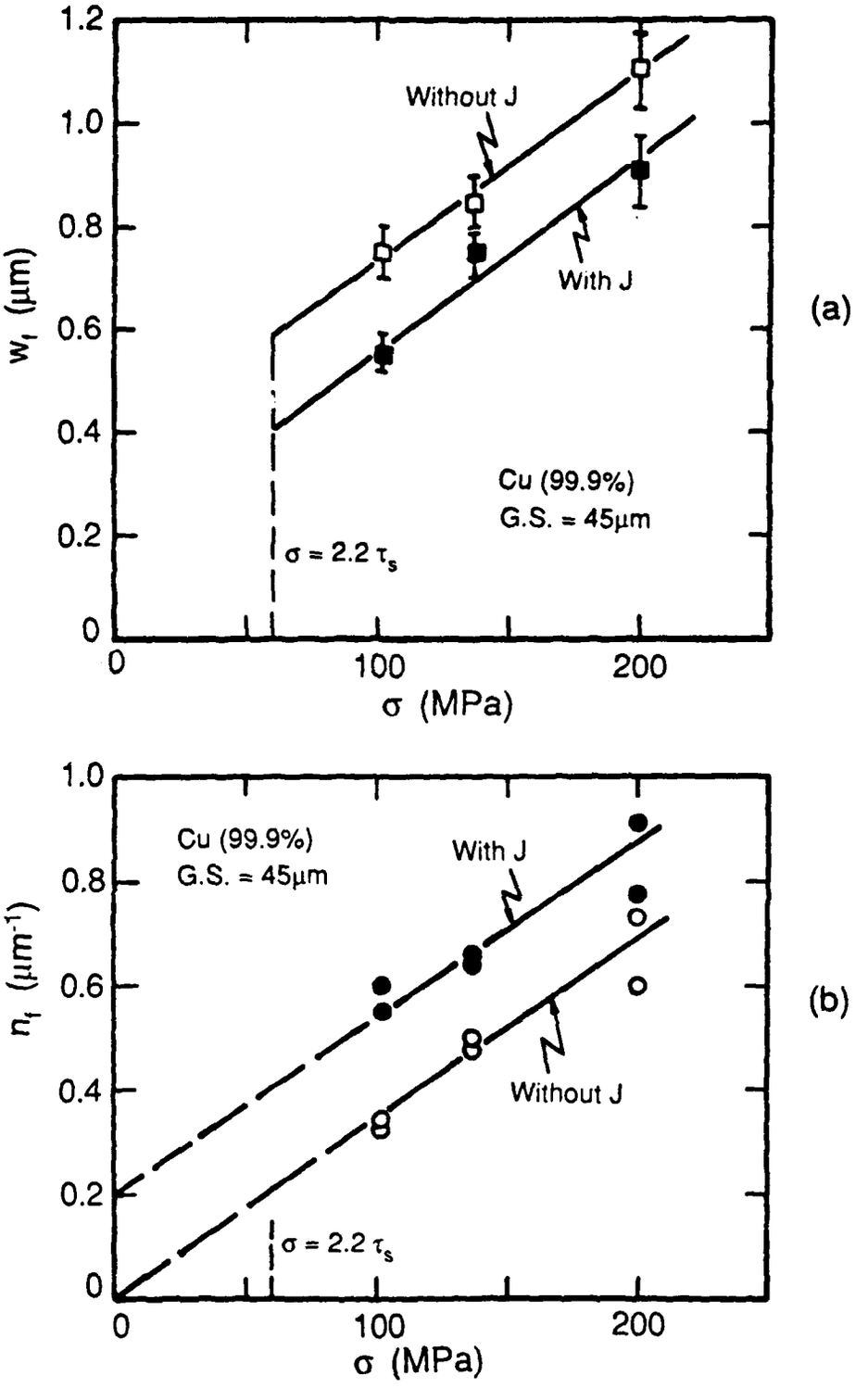

Fig. 9. *Effect of electropulsing* ($j = 1.3 \times 10^4$ A/cm^2, $t_p = 100$ μs, $\nu_p = 2$ Hz) on the linear PSB density n_f and width w_f at fracture as a function of stress. From Conrad et al [37].

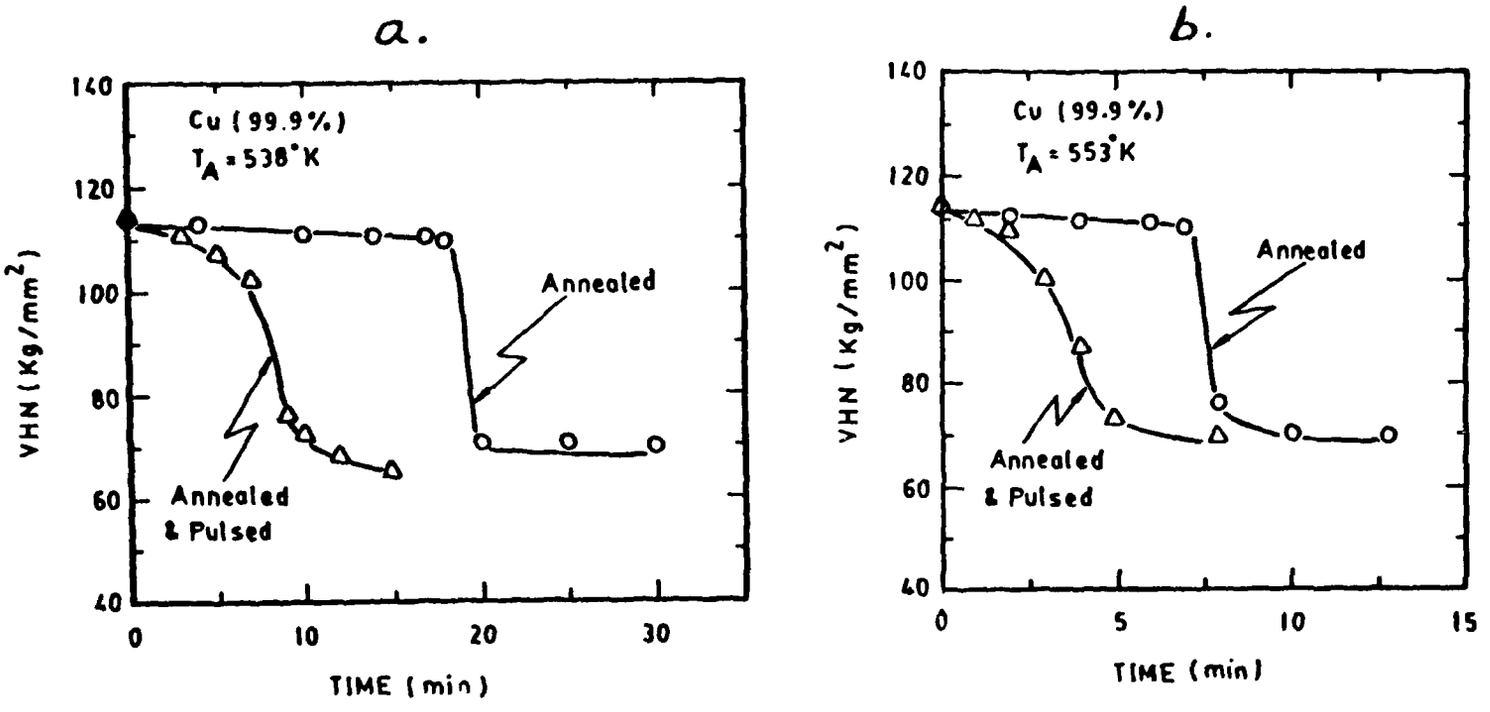

Fig. 10. Effect of electropulsing (j = 8 x 10^4 A/cm^2, t_p = 90 μs, ν_p = 2 Hz) on the isothermal annealing of cold drawn Cu: (a) T_A = 538K and (b) T_A = 553K. From Conrad et al [39].

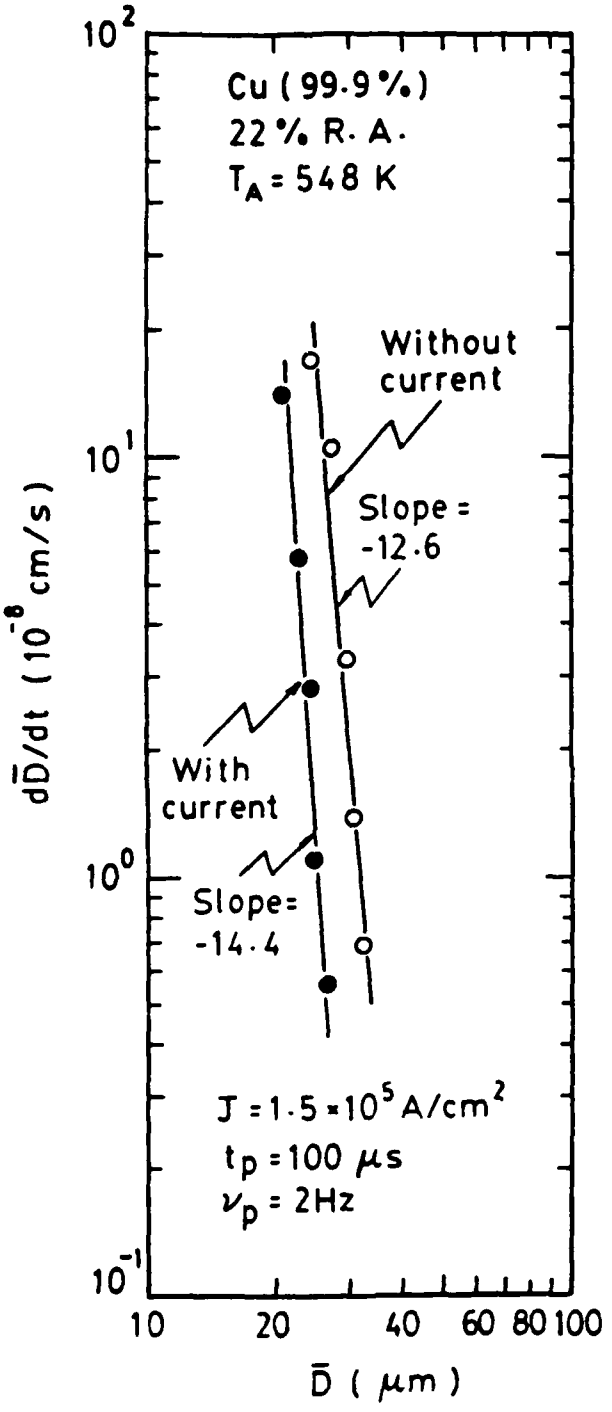

Fig. 11. Effect of electropulsing (j = 1.5 x 10^5 A/cm^2, t_p = 100 μs, ν_p = 2 Hz) on the rate of grain growth dD/dt vs grain size D in Cu. From Conrad *et al* [40].

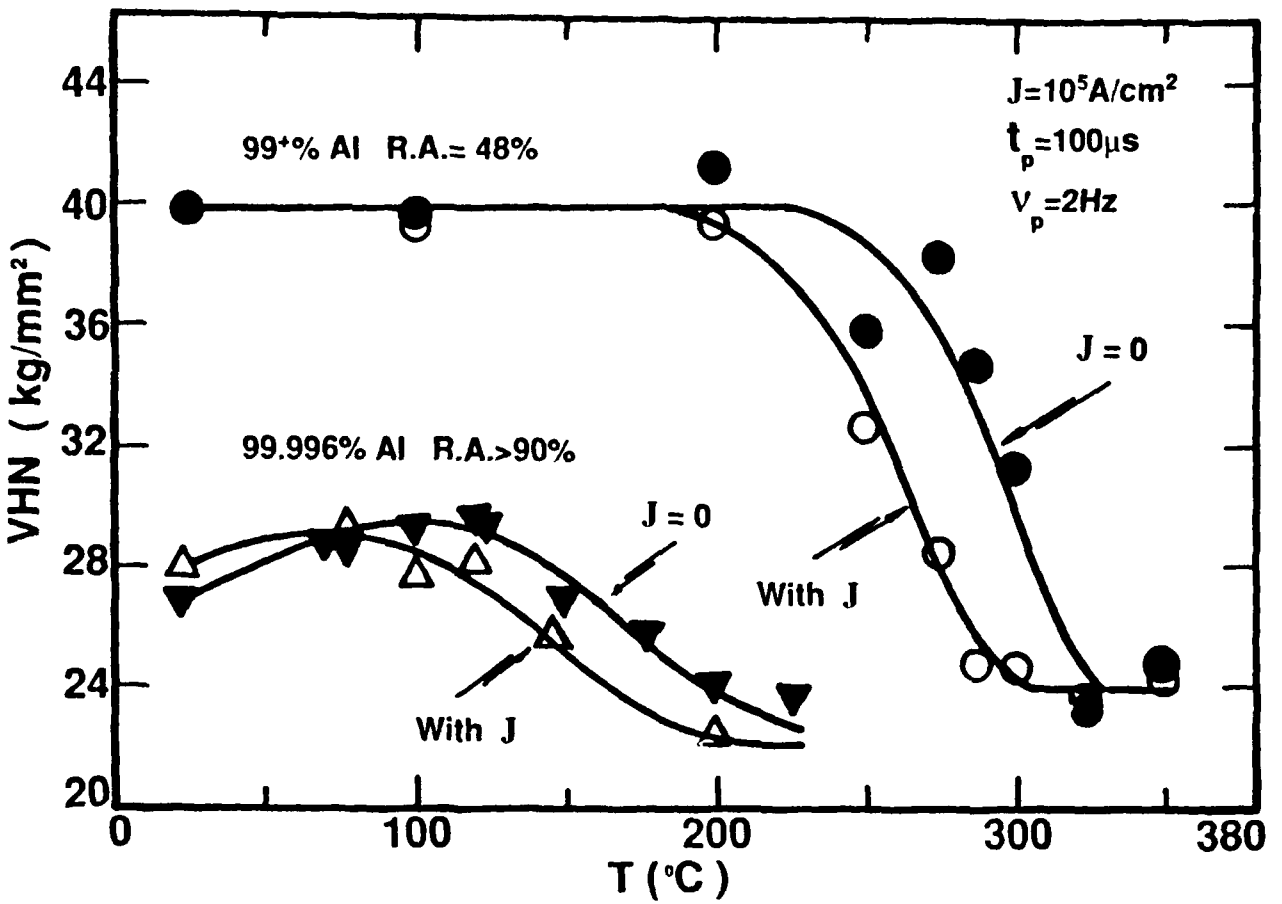

Fig. 12. Effect of electropulsing on the isochronal annealing of Al of two purity levels. Annealing time t_A = 1h.

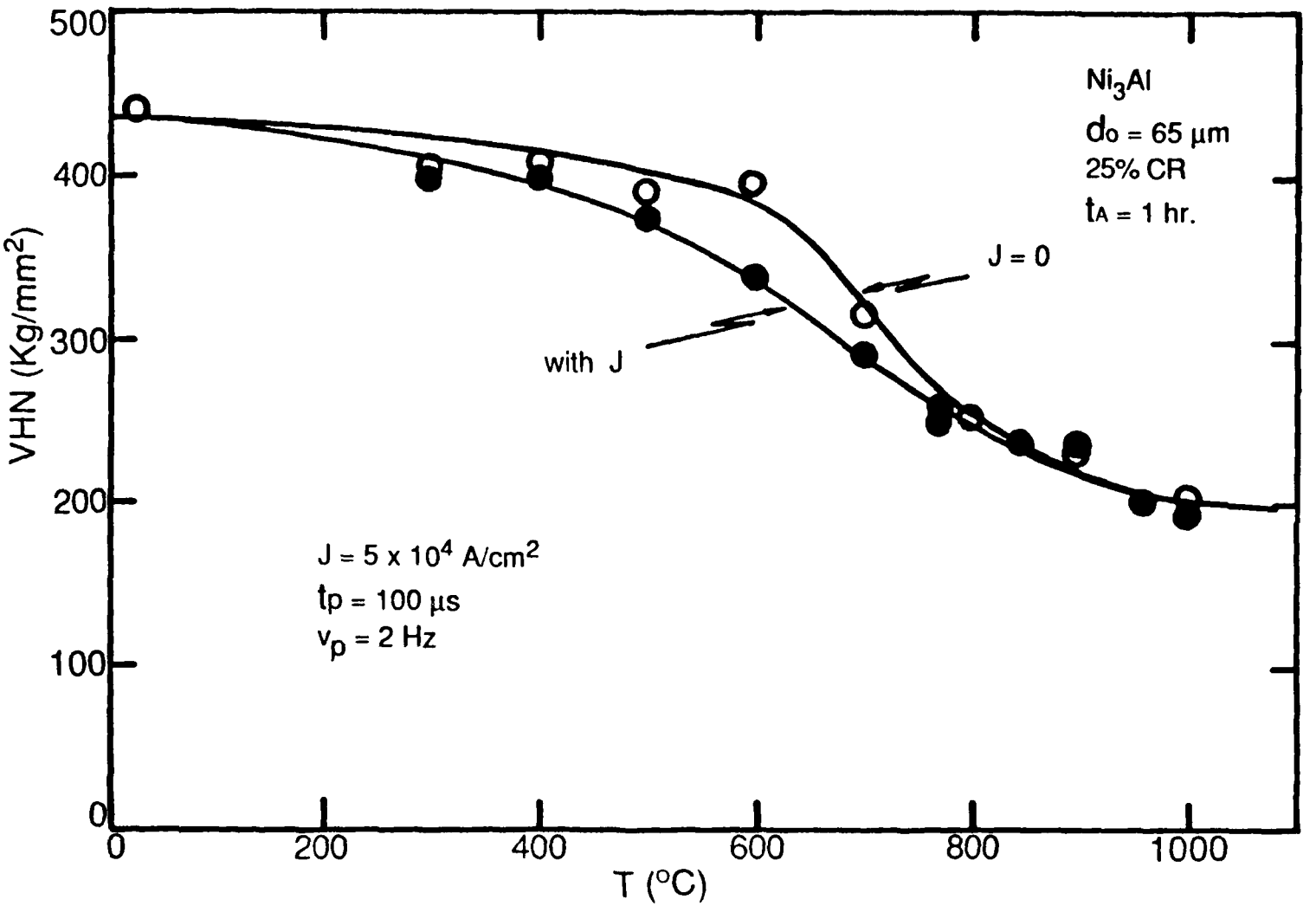

Fig. 13. Effect of electropulsing on the isochronal annealing of the intermetallic compound Ni_3Al cold rolled 25%. Annealing time t_A = 1h.

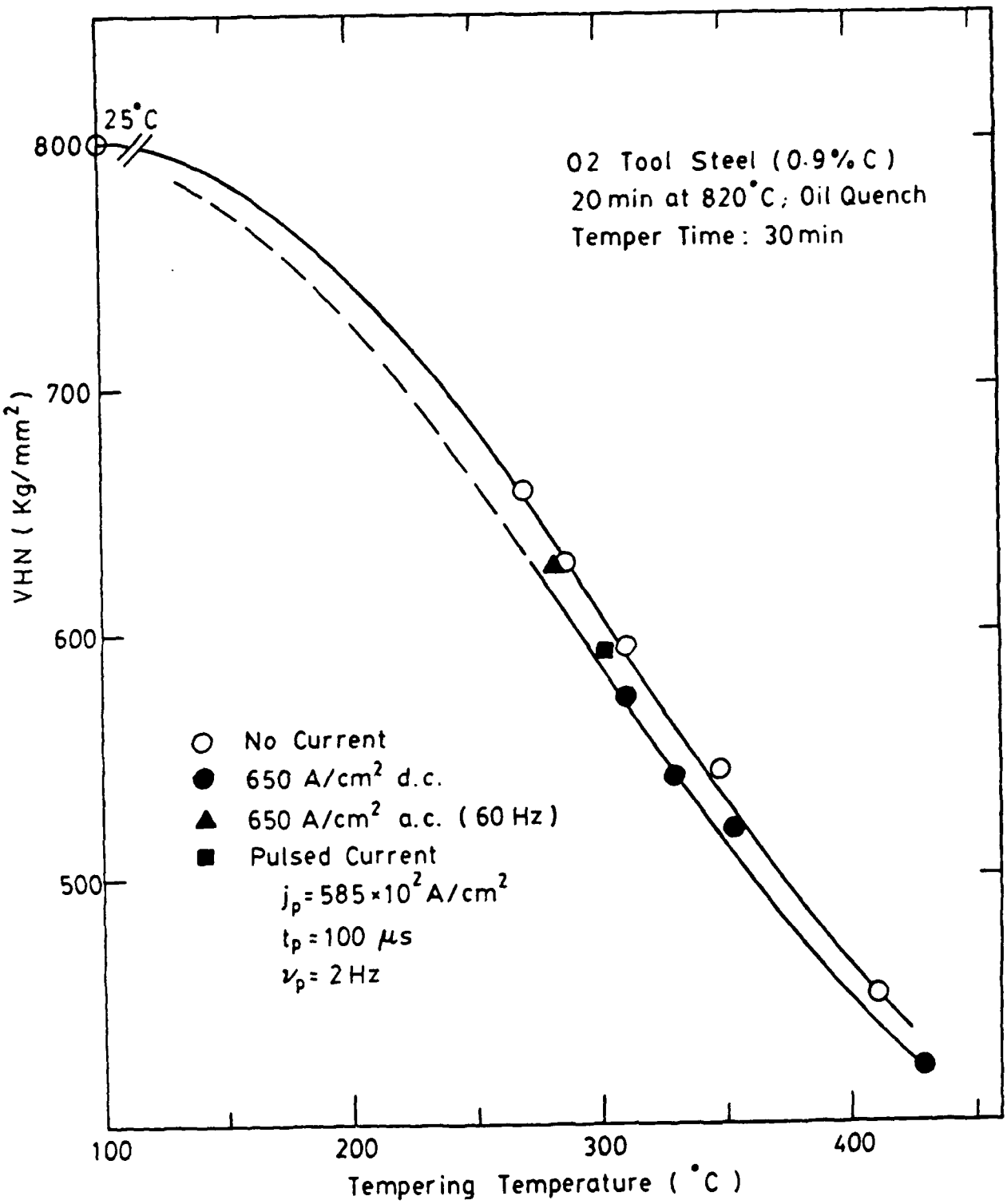

Fig. 14. Effect of **electric current** on the tempering of 02 tool steel.

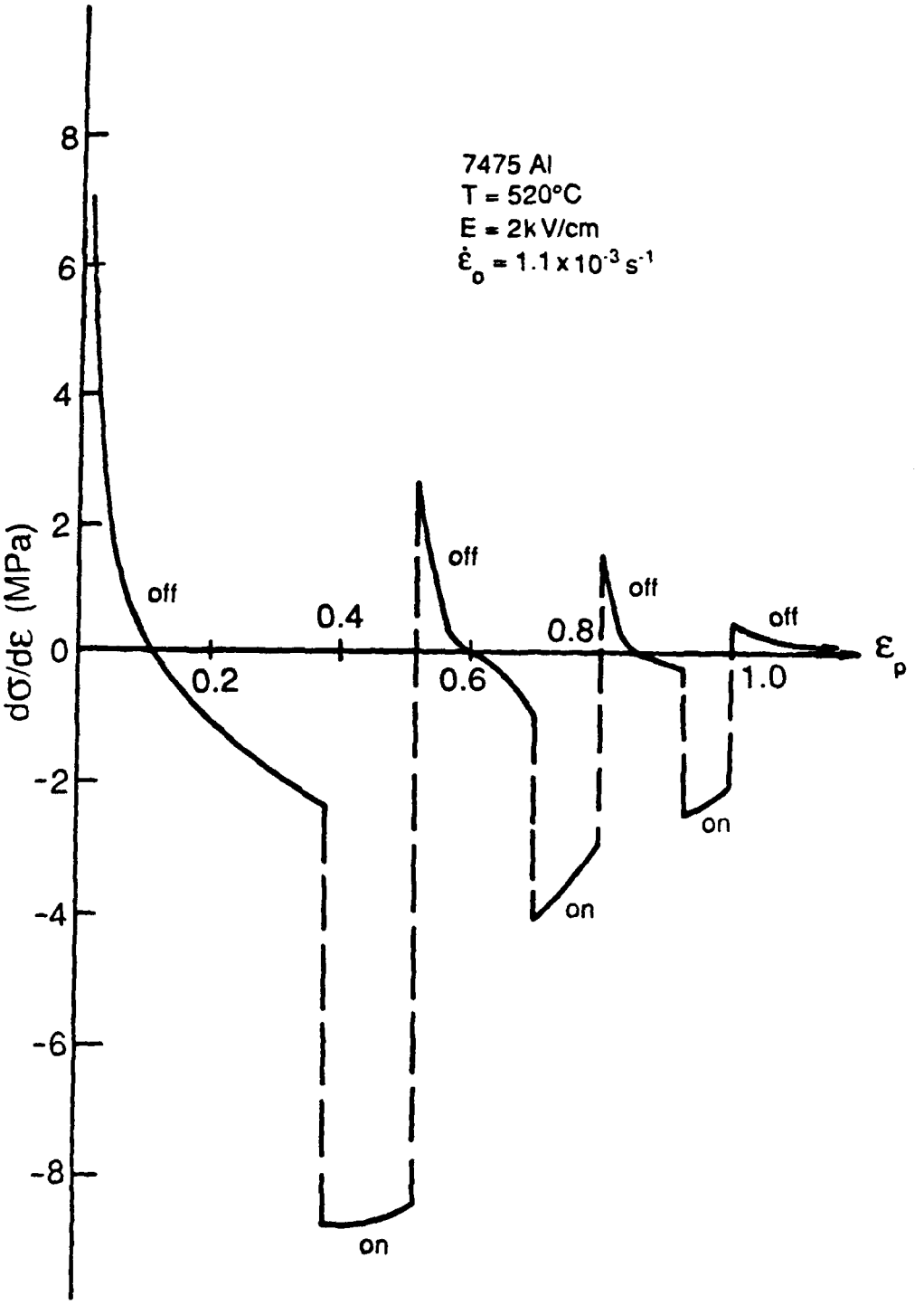

Fig. 15. Changes in the rate of strain hardening when a continuous d.c. electric field E = 2 kV/cm is turned "on" and "off" during superplastic deformation of 7475 Al alloy. From Conrad et al [42].

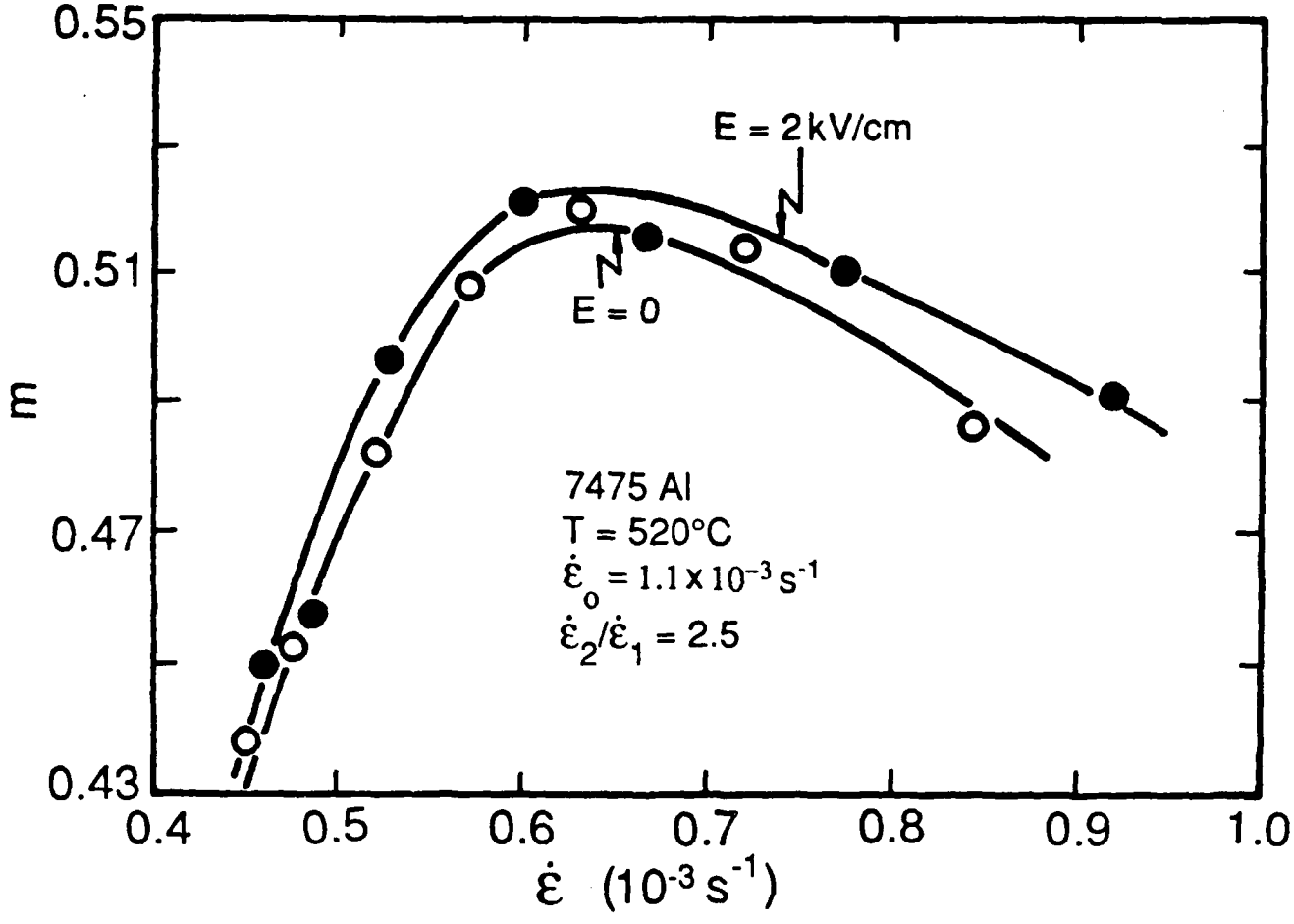

Fig. 16. Effect of a continuous d.c. electric field E = 2 kV/cm on the strain rate hardening parameter m = $d\ln\sigma/d\ln\dot{\varepsilon}$ vs strain rate $\dot{\varepsilon}$ during superplastic deformation of 7475 Al alloy. The variation in $\dot{\varepsilon}$ results from the elongation of the specimen during plastic deformation at a constant crosshead speed. From Conrad et al [42].

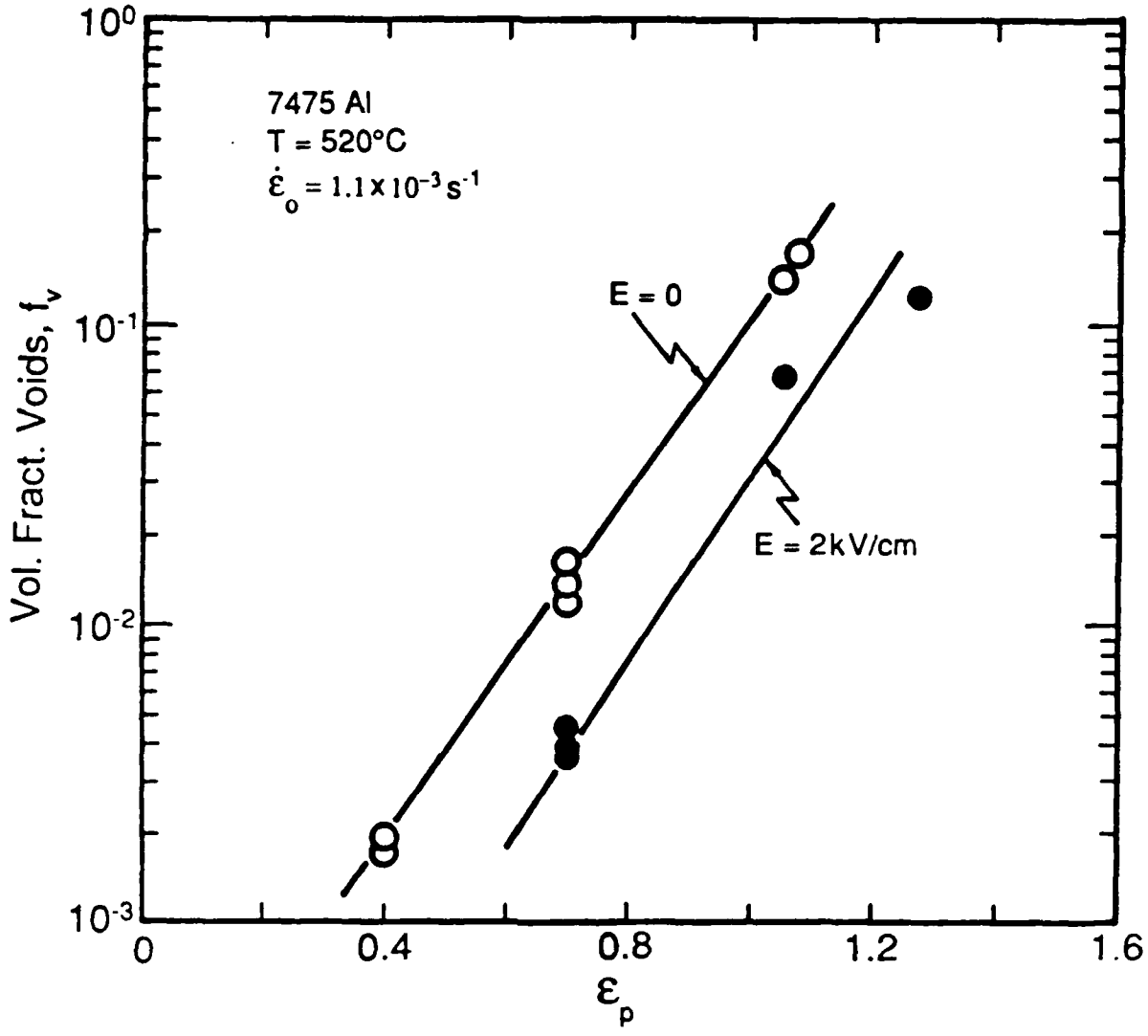

Fig. 17. Effect of a continuous d.c. electric field E on the volume fraction of cavities which develop during the superplastic deformation of 7475 Al alloy From Conrad et al [42].

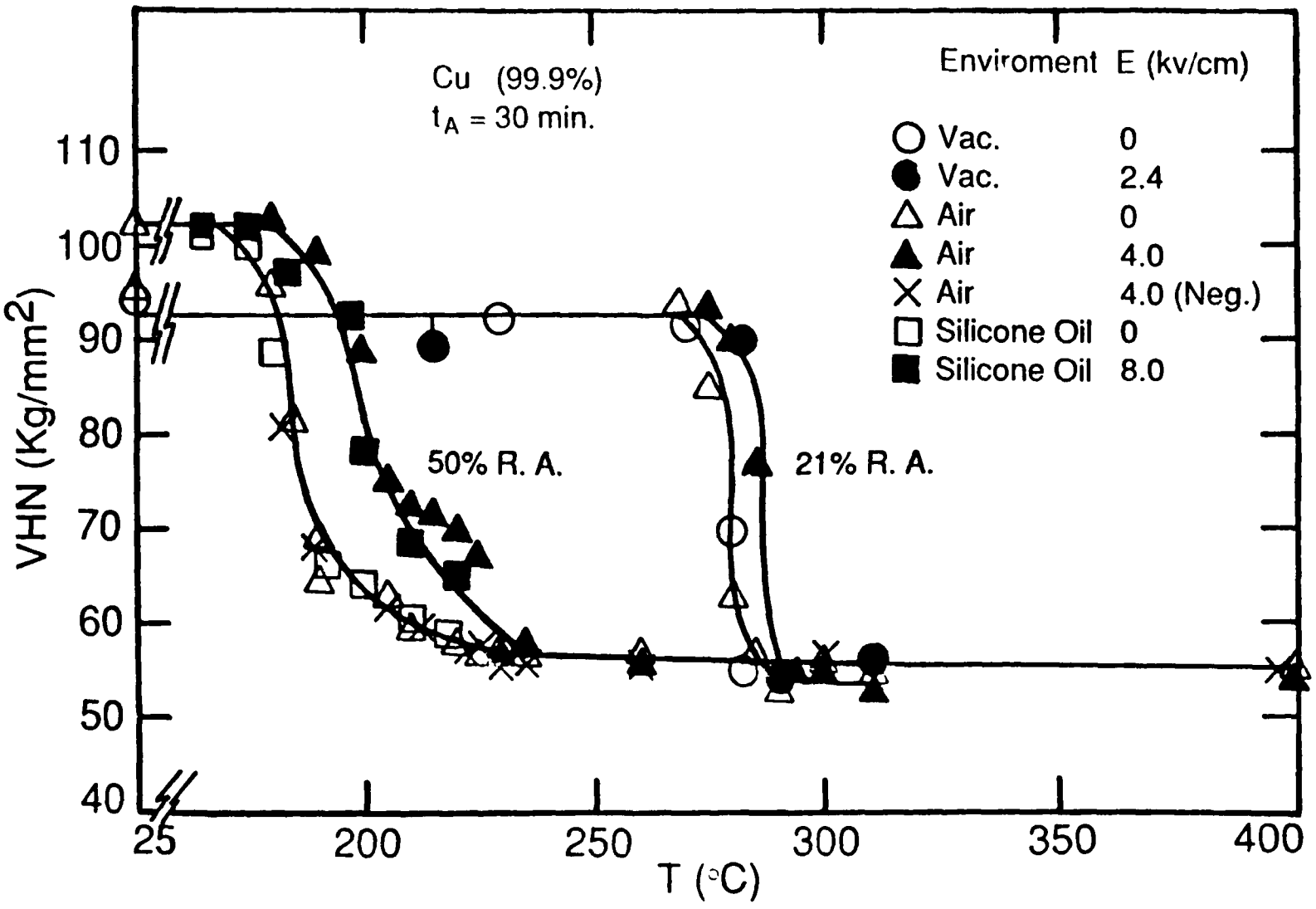

Fig. 18 Effect of a continuous d.c. electric field on the isochronal annealing of Cu in several environments as a function of the amount of prior cold work. From Conrad, Guo and Sprecher [43].

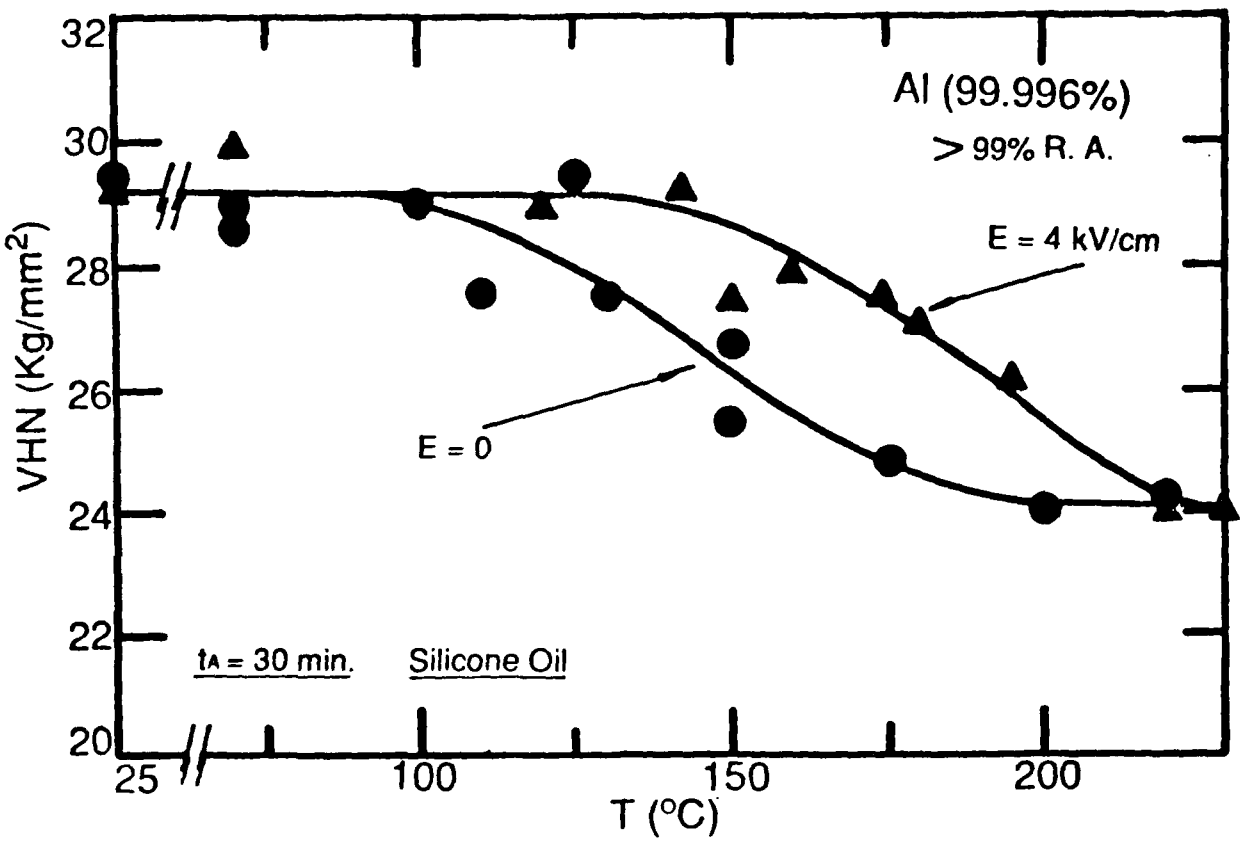

Fig. 19. Effect of a continuous d.c. electric field on the isochronal annealing of severely cold drawn Al heated in silicone oil. From Conrad, Guo and Sprecher [43].

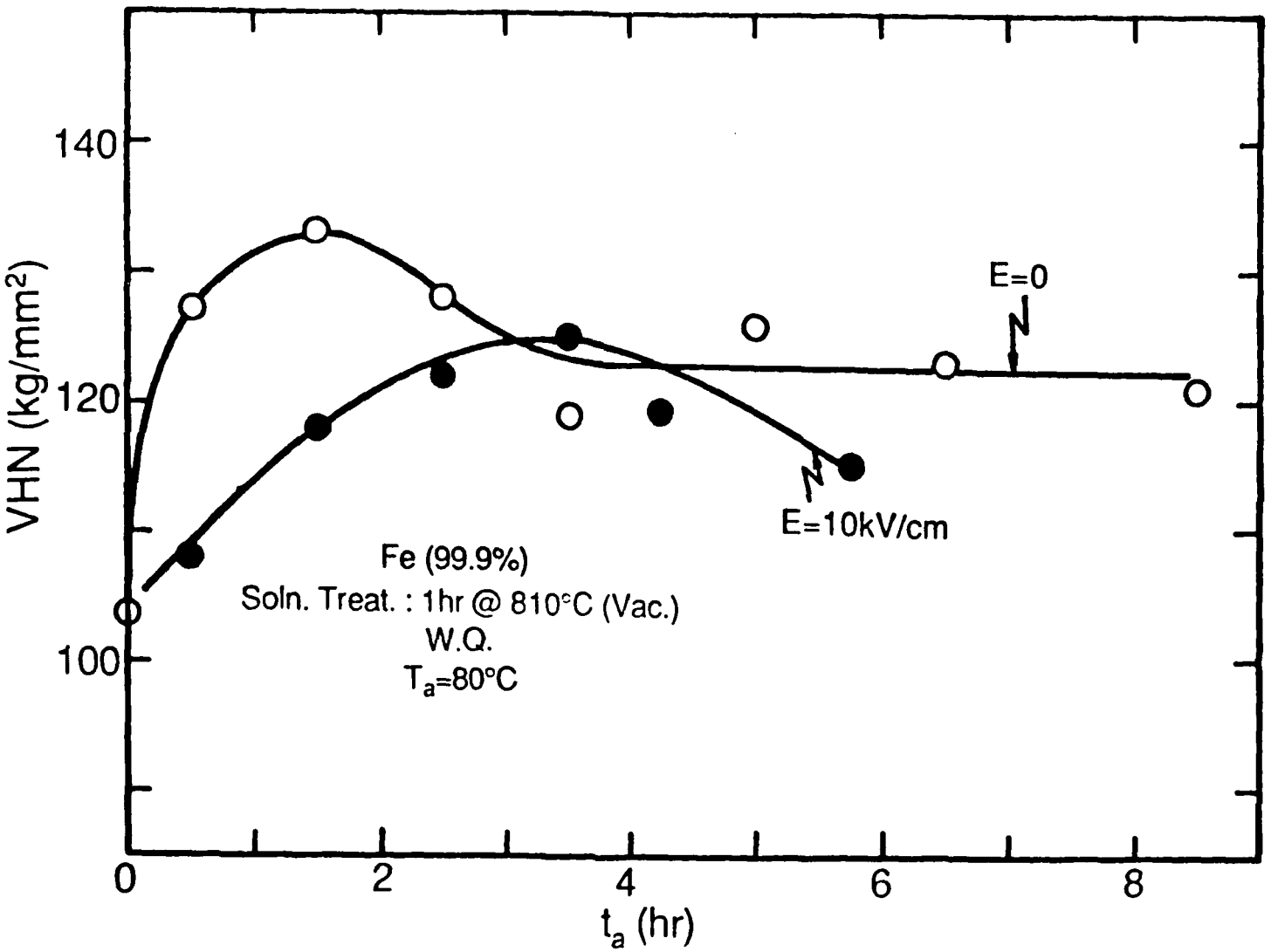

Fig. 20. Effect of a continuous d.c. electric field on the quench again of a low-carbon iron.

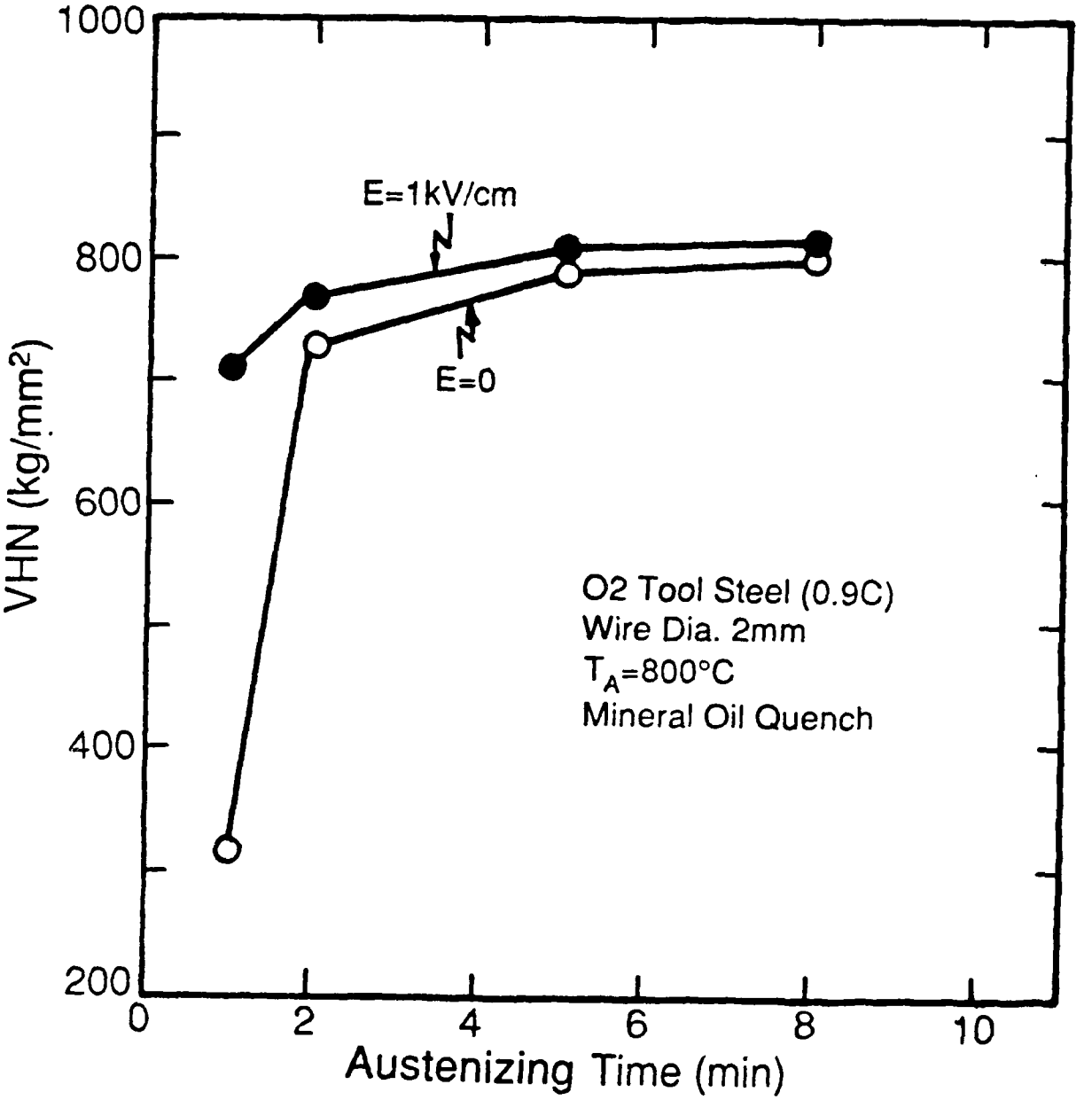

Fig. 21. Effect of a continuous d.c. electric field on the rate of austenizing of an 02 tool steel subsequently quenched in mineral oil. Plot gives hardness of the quenched steel vs austenizing time. From Cao et al [44].

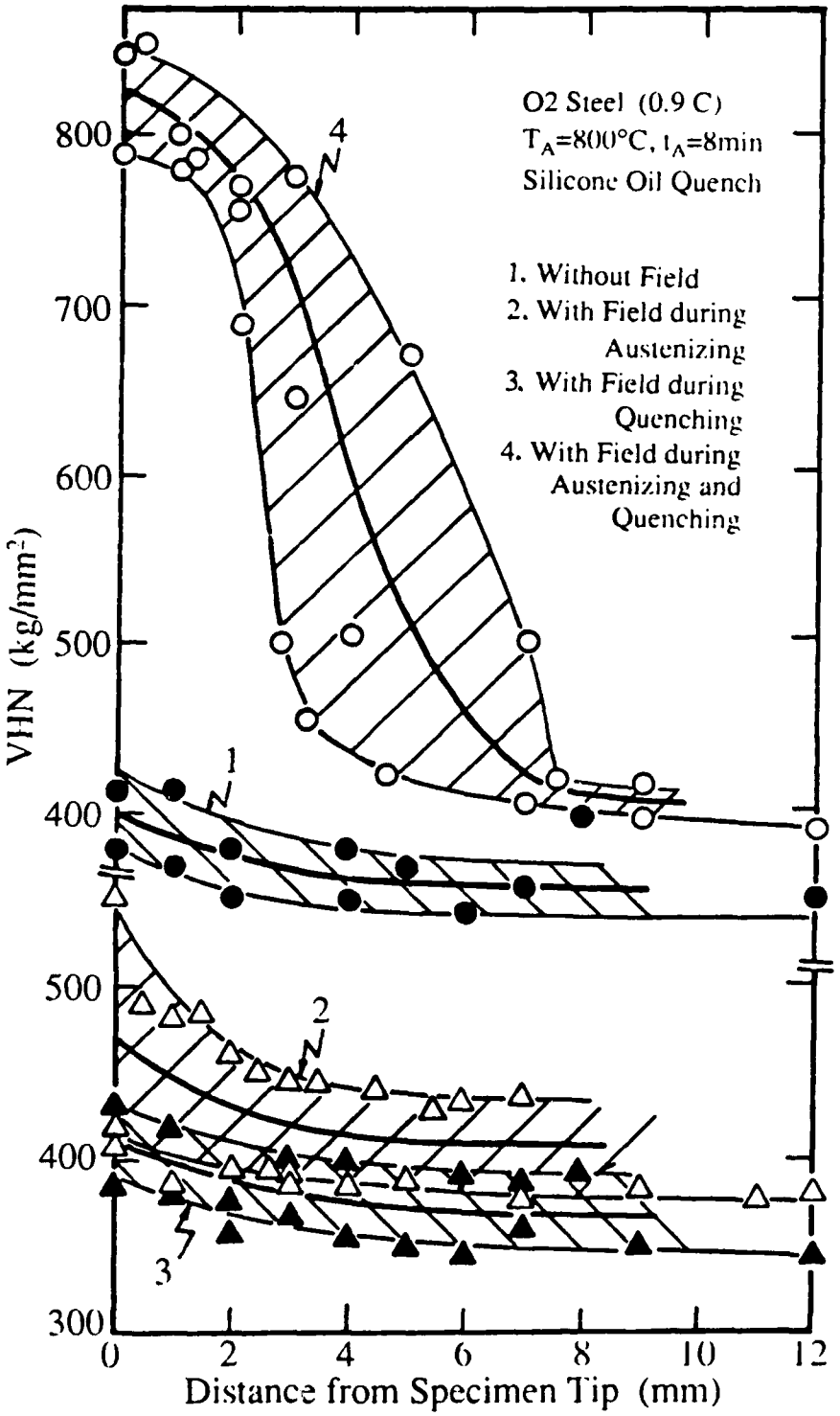

Fig. 22. Effect of a continuous d.c. electric field applied in various combinations during austenizing and quenching on the hardness of a 0.9 C tool steel. From Cao et al [44].

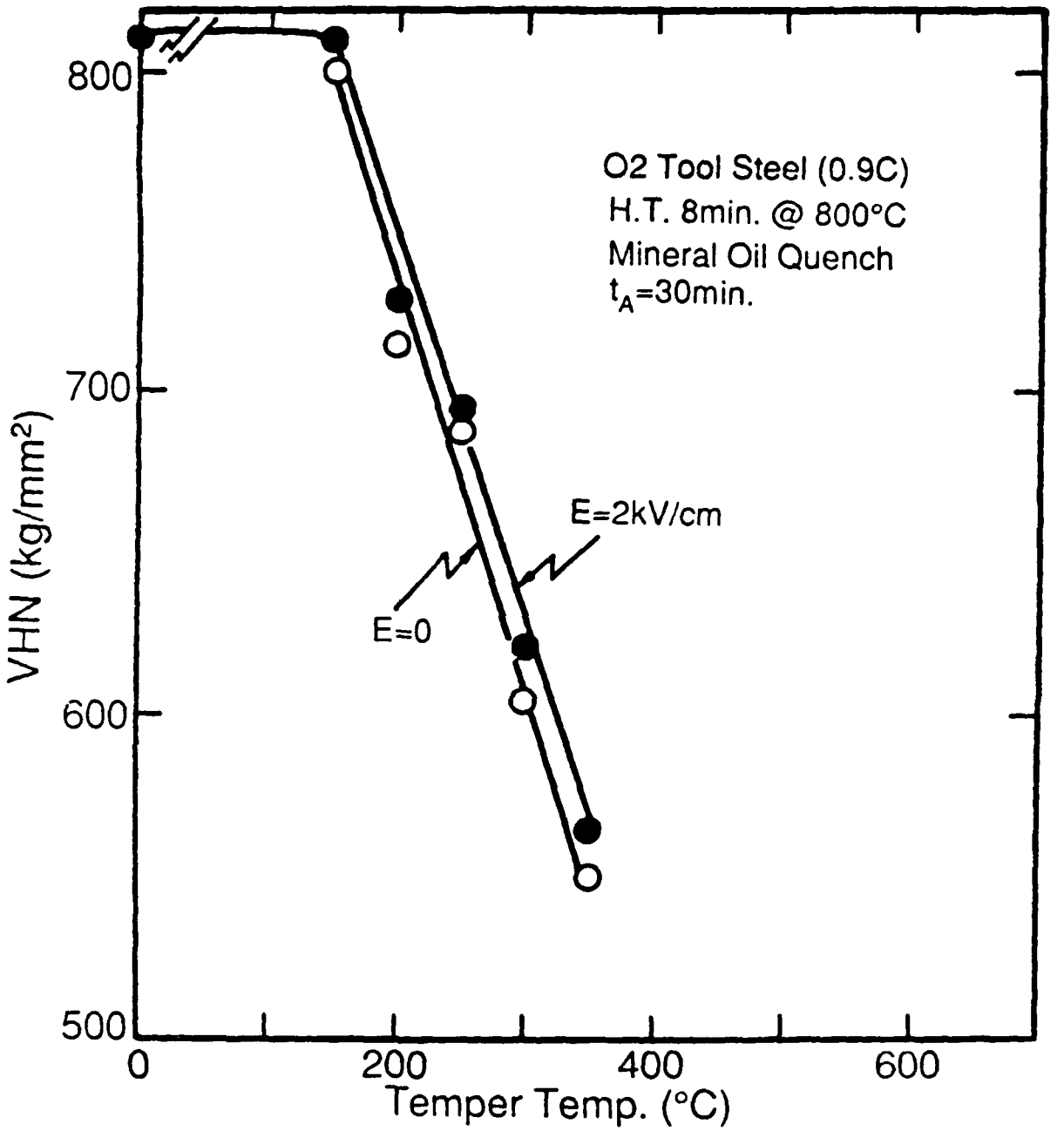

Fig. 23. Effect of a continuous d.c. **electric field** on the tempering of an 02 tool steel quenched in mineral oil. From Cao et al [44].

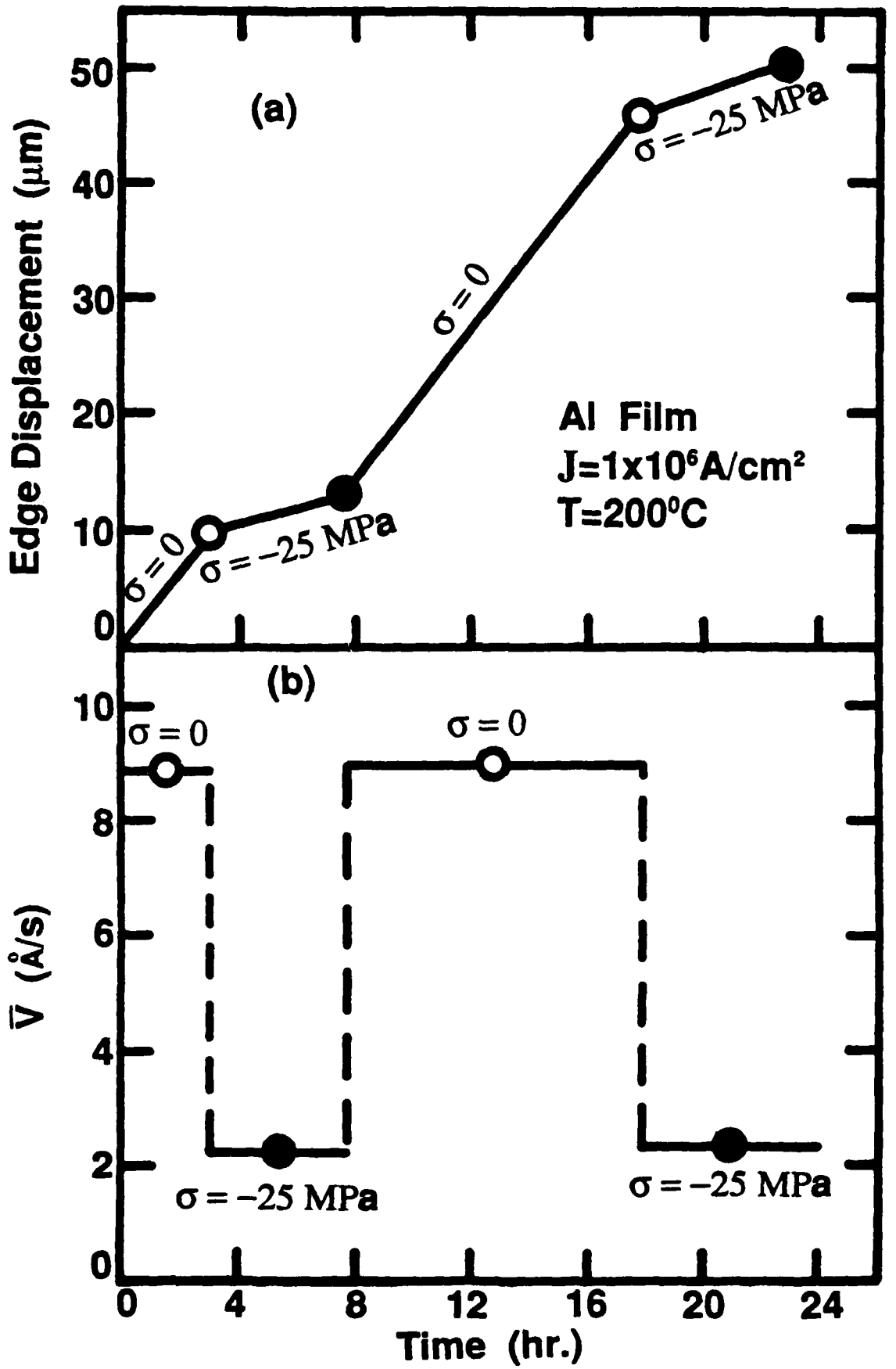

Fig. 24. Effect of a compresive stress of 25 MPa on electromigration in an Al film at 200° C and j = 1 x 10^6 A/cm^2: (a) Displacement of the cathode edge vs time as the stress is changed and (b) The average velocity of the cathode edge derived from the data in (a).